

### **CRITICAL REVIEW**

View Article Online
View Journal | View Issue



Cite this: Analyst, 2023, 148, 1633

# Semiconductor quantum dots in photoelectrochemical sensors from fabrication to biosensing applications

Anjum Qureshi, \* Tayyaba Shaikh and Javed H. Niazi\*\*

Semiconductor quantum dots (QDs) are a promising class of nanomaterials for developing new photoelectrodes and photoelectrochemistry systems for energy storage, transfer, and biosensing applications. These materials have unique electronic and photophysical properties and can be used as optical nanoprobes in displays, biosensors, imaging, optoelectronics, energy storage and energy harvesting. Researchers have recently been exploring the use of QDs in photoelectrochemical (PEC) sensors, which involve exciting a QD-interfaced photoactive material with a flashlight source and generating a photoelectrical current as an output signal. The simple surface properties of QDs also make them suitable for addressing issues related to sensitivity, miniaturization, and cost-effectiveness. This technology has the potential to replace current laboratory practices and equipment, such as spectrophotometers, used for testing sample absorption and emission. Semiconductor QD-based PEC sensors offer simple, fast, and easily miniaturized sensors for analyzing a variety of analytes. This review summarizes the various strategies for interfacing QD nanoarchitectures for PEC sensing, as well as their signal amplification. PEC sensing devices, particularly those used for the detection of disease biomarkers, biomolecules (glucose, dopamine), drugs, and various pathogens, have the potential to revolutionize the biomedical field. This review discusses the advantages of semiconductor QD-based PEC biosensors and their fabrication methods, with a focus on disease diagnostics and the detection of various biomolecules. Finally, the review provides prospects and considerations for QD-based photoelectrochemical sensor systems in terms of their sensitivity, speed, and portability for biomedical applications.

Received 14th October 2022, Accepted 12th February 2023 DOI: 10.1039/d2an01690g

rsc.li/analyst

#### 1. Introduction

Nanoscience research, particularly in the field of bioanalysis, has greatly contributed to the advancement of disease diagnostics and pharmaceutical drug analysis. Piosensors and biodevices incorporating nanoparticles (NPs) have been extensively studied due to their rapid, specific and sensitive responses to the detection of disease biomarkers, drugs, as well as environmental pollutants. Nanomaterials including nanoparticles, nanotubes, nanowires, nanoprisms, and quantum dots (QDs) have been widely studied to improve the performance of biosensors in achieving lower detection (LOD) limits and enhancing sensitivity. Detection mechanisms in biosensors are mainly categorized based on transducing signal formats, such as electrochemical, electrical and optical (fluorescence, absorbance, Raman and surface plasmon resonance

Sabanci University, SUNUM Nanotechnology Research and Application Center, Orta Mah, Tuzla 34956, Istanbul, Turkey. E-mail: javed@sabanciuniv.edu, anjum@sabanciuniv.edu; Tel: +90 216 483 9879/2441

spectroscopy).5 Electrochemical sensors are most widely used and preferred due to their ability to transform biomolecular interactions into an analytically measurable signal, such as a change in voltage or current. Recently, a less well-known technique called photoelectrochemical sensing has emerged, which relies on electrochemical transduction for bio- and chemical sensing, energy storage and energy harvesting due to its ability to covert bio/chemical energy into an electrical signal/energy under an applied potential and light illumination.<sup>6</sup> Photoelectrochemical sensing is a cost-effective approach that combines both optical and electrochemical sensing mechanisms through the conversion of photons to electricity and electrochemical reactions. In PEC sensing, the transducing biomolecular interaction is measured by recording the photocurrent generated due to the oxidation/reduction of biomolecules upon light irradiation. A typical photoelectrochemical (PEC) biosensor consists of a photoelectrode that generates a photocurrent signal upon light illumination through the transfer of electrons between the electrode and analyte molecules. PEC analysis has several advantages, such as high sensitivity, low background noise, and ease of minia-

turization, because it utilizes external excitation energy (light) that transduces the photocurrent signal. However, the mechanism of PEC biosensing platforms relies on the type of nanomaterial interfaced with the PEC electrode, which directly affects the separation, generation, and transport of the photoexcited charge carriers at the nano-bio interfaces.

Recent advances in solar cell research have resulted in the development of numerous new photoactive materials. These organic, inorganic and semiconductor functional materials can be used not only in solar cells and energy-harvesting but also in photoelectrochemical Photoelectrochemistry is the conversion of optical light into electrochemical energy through the reaction between photoactive organic, inorganic, and/or semiconducting materials. There are several categories of photoactive material that have been used in PEC sensing, such as transition metal complexes like Ru(bpy)<sub>3</sub><sup>2+</sup> and its derivatives, <sup>9,10</sup> organic materials such as phthalocyanines, <sup>11</sup> phenothiazine, <sup>12</sup> porphyrins, <sup>13</sup> and conductive polymers, <sup>14</sup> and inorganic semiconductors such as zinc oxide (ZnO), titanium oxide (TiO2), and tungsten oxide (WO<sub>3</sub>). Additionally, certain nanomaterials, such as TiO<sub>2</sub> nanoparticles and nanotubes, graphene oxide (GO), graphitic carbon nitride  $(g\text{-}C_3N_4)$ , and semiconductor nanoparticles have been recognized as transducing elements in the fabrication of PEC sensors. 16,17 The use of photocatalytic materials in PEC has been previously reviewed, and the advantages of integrating photoactive materials have been documented in the literature. 18 However, the fabrication of photoactive materials for use in biosensing applications is challenging due to low sensitivity, high cost, poor signal amplification and difficulties in applying them for point-of-care (PoC) devices.

QDs with sizes ranging from 2 to 10 nanometers are highly sought-after nanomaterials in nanotechnology because of their particle size, tunable emission based on composition, broad excitation and absorption range, narrow and symmetrical photoemission, strong luminescence, and robust photostability. They are promising alternatives to organic fluorophores in the development of new-generation photoelectrodes and photoelectrochemical biosensors. QDs have size-dependent optical properties and unique optical and photoelectrical characteristics that make them useful for PEC biosensing. When used in PEC biosensing, QDs generate a photocurrent that is sensitive to the chemical environment of the surrounding solution. 19 QDs are semiconductor nanocrystals typically made of elements from group II/VI (such as CdSe, CdTe, CdS), or III-V (InAs, GaAs), or IV-VI (PbS, PbSe).20 QDs that are derived from group II/VI elements (such as CdSe and CdTe) have inherent cytotoxicity due to the presence of the individual ions, such as Cd2+, Se2-, and Te2-. To address the toxicity, core-shell QDs are synthesized which consist of a luminescent semiconductor core surrounded by a thin shell of a higher bandgap element. For example, a thick shell of ZnS is often grown over CdSe or CdTe nanoparticle cores, making them less toxic compared with the ions in the core dots. The outer ZnS shell acts as a barrier that prevents the core (CdSe) from coming into contact with the surrounding solvent and dissolving due to ionization. The outer shell also increases the quantum yield by passivating non-radiative recombination sites on the core surface. Semiconductor QDs based on the elements of group III-V are generally less toxic and more stable due to the presence of a covalent bond, as compared with the ionic bond in semiconductor ODs based on elements from group II-VI. QD-interfaced PEC sensors have gained widespread interest as an alternative organic fluorophore in biological applications due to their luminescence and ability to glow when excited by a specific wavelength light source. These characteristics offer significant advantages over conventional organic dyes. Many reviews have been published that extensively cover a variety of nanomaterial-based PEC sensors and their applications. 11,14,21 For example, Zang et al. 11 published a review article on the advancement of a graphitic carbon nitride (g-C<sub>3</sub>N<sub>4</sub>) and transition-metal dichalcogenide (TMD), and QD-based photoelectrochemical sensor application. Another review provided a brief overview of the PEC principle, mechanism, and applications, and also focused on semiconductors, dyes, composite semiconductor-semiconductor materials, and hybrid dve-semiconductor materials.21 Recently, Yang et al.14 reviewed a variety of nanomaterials, such as QD modifications, and metal/non-metal ion doping, for use in photoelectrochemical sensors. The role of QDs as versatile energy transfer donors and acceptors in biological configurations and applications has been reviewed in previous publications.22 However, unlike other reviews, the current review is more focused on the practical approaches to fabricating different types of QD-interfaced PEC sensor electrode, with an emphasis on the role of QDs in PEC sensing, improving photophysical properties through different designs of heterojunction approaches, and the applications of photoelectrochemical biosensor devices for disease diagnostic and biosensing applications.

# 2. Basic principle of a photoelectrochemical sensor

The basic principle of a photoelectrochemical sensor is that it relies on the ejection of carrier charges from a photoactive surface upon illumination by light, which causes a photoelectric effect that generates electrical signals.<sup>23</sup> PEC biosensors combine photochemistry and biosensing, where light is used to stimulate the surface of a photoactive material which is used to the immobilize biomolecules (receptors) on its surface that serve as biorecognition entities to specifically capture the target analyte and facilitate the transfer of electrons with enhanced signal amplification. 14 In general, the working electrode in PEC sensing is either fabricated or modified using a photoactive semiconductor material capable of generating electron-hole pairs at the interface upon irradiation by a light source (Fig. 1).24 The photogenerated electron-hole pair participates in the redox reaction process in the aqueous solution, converting light into an electrical signal. There are three main components of PEC sensing systems, namely: (i) an excitation

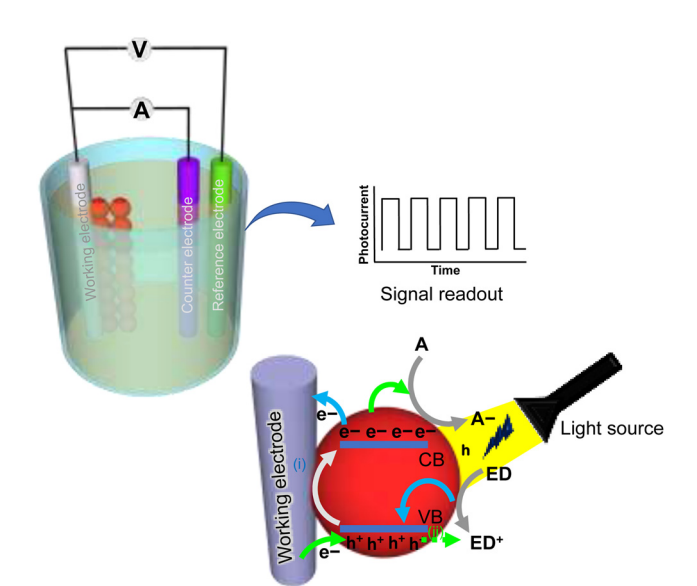


Fig. 1 Schematic illustration showing the basic components of a photoelectrochemical sensor made of a three-electrode system with a signal readout component. Upon illumination of a photoactive material such as semiconductor QDs with light, electron-hole pairs are generated. As a result of light excitation, excited electrons (e<sup>-</sup>) move from the valence band (VB) to the conduction band (CB) in the QD, leaving behind positively charged holes (h<sup>+</sup>) in the VB. When electrons from the CB of a QD move to a positively charged electrode, the holes in the VB of the QDs consume electrons from an electron donor (ED) to neutralize the holes in the VB, and as a result an anodic photocurrent is generated. On the other hand, when electrons in the conduction band are electrostatically attracted to a solution-soluble electron acceptor (A<sup>-</sup>), the supply of electrons from the electrode to neutralize holes in the VB of the QDs results in the generation of a cathodic photocurrent.<sup>14</sup>

light source, (ii) a signal converter that generates and transfers the carrier charges towards the electrodes, such as a working electrode modified by a photoactive material, electrolyte, and biomolecules, and (iii) an electrical signal readout system.<sup>5</sup>

The selection of a photoactive material with high photoconversion efficiency is critical in PEC sensing because this material serves as a photoelectrode to generate electron-hole pairs and transduce the chemical information from an analyte-induced interaction into a readable PEC/photocurrent signal.<sup>25</sup> In PEC phenomena, the absorption of photons with energy  $\geq E_g$  (bandgap energy) of a photoactive material leads to the formation of an exciton (electron-hole pair). When light excites a photoactive material, photoexcited electrons move from the VB to the CB, leaving behind holes in the VB. To generate an electrical signal, the photogenerated charge carriers (electrons-holes) must travel to the surface of the bulk material for use at the electrode surface or in electrolyte solution. However, the electron-hole pair has the ability to recombine in certain ways to dissipate the absorbed energy. It takes different time intervals for the migration of the electron-hole pairs to the surface (hundreds of picoseconds) compared with the recombination of electron-hole pairs (several picoseconds), resulting in a large number of carrier recombinations at the surface, and reduced efficiency of the PEC process.<sup>5</sup> Therefore, the design and engineering of the photoactive material are crucial for efficient PEC sensing. There are two types of photocurrent that can be observed due to the movement of carrier charges across the electrodes. A cathodic photocurrent is observed when the light-driven electron from the electron-hole pair in CB is transferred electrostatically towards an electron acceptor species, causing electrons to be provided by the electrode to neutralize the holes in the VB. Conversely, upon light irradiation, the holes in VB may be filled by electrons supplied by electron donor species at the interface of the electrode-solution, resulting in the transfer of electrons from the CB to the electrode, and an anodic photocurrent is generated.<sup>26</sup> Typically, the PEC sensor can either be a 'signal-on' or 'signal-off' type. In 'signal-on' settings, the analyte-induced redox reactions at the electrode interface lead to the electron transfer, and the levels of analyte present are directly proportional to the photocurrent signal. In contrast, the 'signal-off' mode of PEC sensor involves the formation of a barrier because of an analyte-mediated biorecognition reaction occurring at the electrode surface, which can either generate steric hindrance or inhibition of the redox species. These hindrance effects prevent mass and electron transfer at the surface of the electrode, which lead to a reduction in the photocurrent. The 'signal-off' mode of PEC sensing follows an inverse relationship with the concentration of the analyte. The specific role of semiconductor-based QDs in PEC sensor development is discussed in following section.

# 3. Role of semiconductor quantum dots in PEC sensing

In PEC sensing, QDs can be used as the active component of a conductive photoelectrode, which generates an electrical or photocurrent output signal in response to changes in the chemical environment of the surrounding solution. In PEC sensing, QDs can act as a photoactive charge carrier pump on a conductive electrode by initiating charge transfer between the electrode and the redox species in solution. This process is typically facilitated through tunneling processes, where the charges are transferred trough the bandgap of the semiconductor material. As a result, the PEC sensor can generate a high signal sensitivity and fast response, making it an effective tool for a variety of applications.

The bandgap of the QD nanocrystals is largely affected by their size, which in turn affects their photoluminescence and electrical properties.<sup>27</sup> When the size of a semiconductor nanocrystal is less than twice the Bohr radius of the excitons (electron-hole pairs), the semiconductor exhibits a phenomenon known as quantum confinement.<sup>28</sup> This happens when the energy gap in the electronic band structure causes the spatial confinement of electron-hole pairs in one or more dimensions within the material.<sup>29</sup> As the size of the nanocrystal is reduced, quantum confinement leads to discrete energy and electronic states with an increased bandgap energy (Fig. 2).

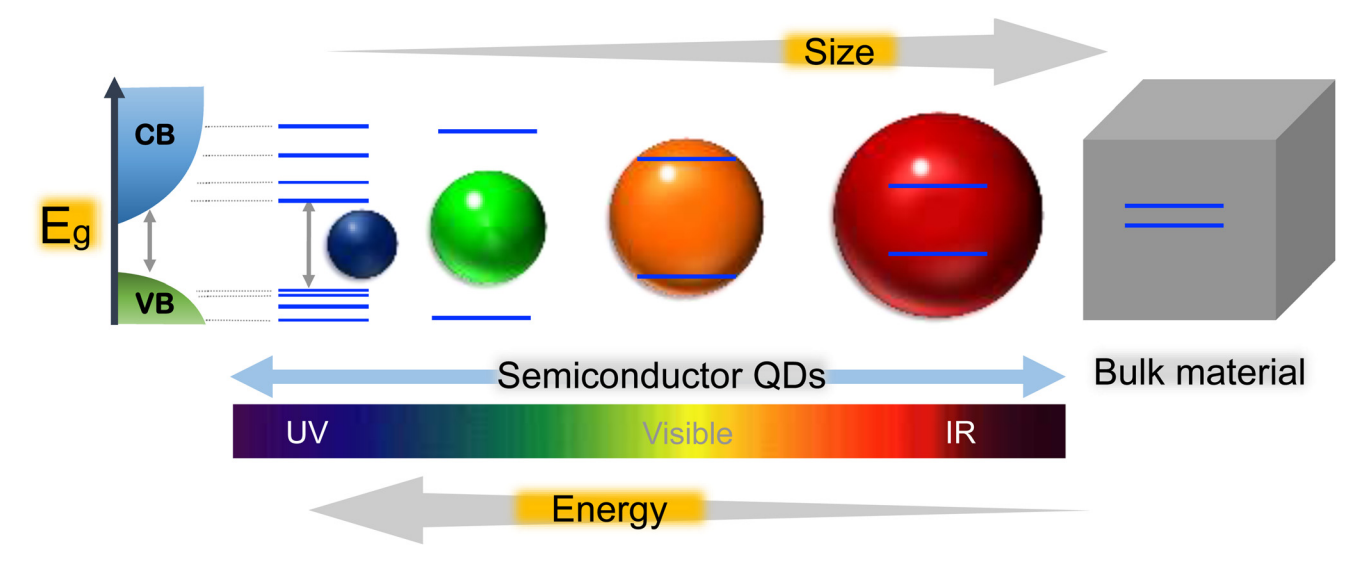


Fig. 2 Schematic illustration of band gap energy  $(E_q)$  variation in bulk material and with different sizes of semiconductor QDs.

In bulk materials, the number of energy states increases significantly, forming nearly continuous bands of states. However, in semiconductor QDs with a 2-10 nm diameter, the confinement of delocalized energy states occurs due to the reduced number of atoms (usually a few atoms to several tens of atoms in diameter) in the material. Electron-hole pairs become spatially confined when the diameter of a particle approaches the de Broglie wavelength of the electrons in the conduction band.30 The small size of semiconductor nanocrystals leads to the confinement of excitons, causing the localized particle to have a broader range of momentum/energy and the average energy of electrons in the conduction band to increase. As a result, the energy difference between energy bands increases, leading to a larger band gap with decreasing particle size. The size-dependent properties of QDs can be used for multichannel detection in a PEC sensor system.

As discussed above, QDs are ideally used as photoelectrochemically active semiconductor nanoparticles because, upon photoexcitation, the electron-hole pairs are generated due to the transfer of electrons from the VB to the CB. In PEC sensing, the photoluminescence properties of QDs play a key role in the radiative charge carrier recombination (electron-hole) or trapping of the electrons in the conduction band. These processes can be controlled through the delays in electron-hole recombination and allow movement of these electrons either towards the electrode surface (due to the presence of reducing molecules as an electron donor in the solution) or the electron accepting species (presence of oxidant molecules) inside a solution to generate the anodic or cathodic photocurrent.<sup>31</sup>

One key advantage of using QDs in PEC sensing is their ability to absorb a wide range of wavelengths of light, which allows them to be excited by a constant wavelength of light and enables the design of simple, inexpensive, miniaturized, and portable sensor platforms. Additionally, the narrow emission spectra of QDs allow for the detection of a specific chemi-

cal species or analyte through the measurement of the emission intensity at a particular wavelength. This can be used to differentiate between different chemical species and allows for the detection of trace levels of specific analytes in complex samples. The facile surface properties of QDs further make them more suitable for efficient chemical coupling with biomolecules and other moieties, which can be used to detect a wide range of biomolecules that cannot be detected using conventional optical methods. Overall, the use of QDs in PEC sensing offers many advantages, including high sensitivity, fast response, and the ability to detect a wide range of chemical species, making it a promising technology for a variety of analytical and medical diagnostic applications.

Several semiconductor metal oxides, such as ZnO, TiO<sub>2</sub>, and WO<sub>3</sub>, were used as photoactive materials to fabricate the electrodes for PEC sensing. Despite TiO<sub>2</sub> being an exceptional photoactive material, widely used for PEC sensing due to its low toxicity, high bandgap energy, and physical and chemical stability, it has certain shortcomings, such as high electronhole recombination rates and low photoconversion efficiency. <sup>26,32</sup> Such limitations can be addressed by the incorporation of a semiconductor QD-based hybrid designs, where the bandgap can be tailored easily and the bandgap energies can be matched by a proper alignment of one or more semiconductors in the vicinity of the QDs.<sup>5</sup>

Also, the correct arrangement of QDs with other semiconductor/conductive electrodes in the design of photoelectrochemical sensors can reduce the working potential and energy consumption. The output photocurrent response of QD-based photoelectrochemical sensors depends on the distance between the QDs and the conductive electrode (the thickness of the conductive electrode), the bandgap distance between the conduction and valence bands of the QDs (dependent on the size and composition of the QDs), the Fermi level position in the conductive electrode (bias potential) and the concentration of redox molecules in the solution.<sup>19</sup> QDs possess a high fluorescence quantum yield and excellent stability against degradation and photobleaching effects.<sup>33</sup>

For the application of QDs in photoelectrochemical sensing, it is also important that minimum surface traps occur on the QD surface because surface traps can reduce the charge transfer rate to the electrode or the redox molecule that can result in a unidirectional photocurrent and the amplitude of the photocurrent will be dependent on the light intensity. These surface traps on the surface of QDs can occur due to a break in symmetry of the QD surface that causes energetic states to appear in the form of vacancies or defects within the band gap of the QDs. 19 The traps on the surface can be minimized by improving the synthesis of QDs in the form of a colloidal suspension and or core-shell-based nanostructure with higher photoluminescence efficiency. Furthermore, QDs also exhibit unique characteristics, such as a high surface-tovolume ratio, good conductivity, and high reactivity, making them suitable candidates for PEC sensing.<sup>34</sup> In the following section, QDs synthesis strategies and their surface modification are briefly discussed, which is useful for developing OD-interfaced PEC sensor devices.

#### 3.1. Colloidal synthesis of QDs

**Analyst** 

QDs can be synthesized using top-down and bottom-up approaches. In top-down strategies, the bulk semiconductor is downsized to form smaller nanocrystals using lithography, etching or laser ablation. Since the top-down approach is not a commonly used method, we limit our discussion to bottom-up techniques, particularly those involving wet chemistry. Colloidal synthesis is the simplest and commonly utilized method for the synthesis of QDs in laboratories. Colloidal synthesis involves the rapid formation of nuclei followed by the slow growth of the nanocrystals. The rapid nuclear growth is accomplished by the introduction of precursors into the reaction mixture containing the hot organic solvents.<sup>2,35</sup> A variety of solvents and their mixtures are employed for the colloidal synthesis of QDs, including phosphine and phosphine oxides, fatty acids, ethers, phosphonic acids and alkenes. QDs can be tailored to the desired sizes by optimizing the reaction temperature, the time for their growth and the choice of solvent medium<sup>2</sup> (Fig. 3a). High-quality monodispersed QDs with specific average sizes can be synthesized in large quantities using a colloidal synthesis method. 2,34,36

#### 3.2. Ligand exchange, solubilization and bioconjugation of QDs

The commonly employed process for QD synthesis involves the use of coordinating organic solvents, such as trioctylphosphine oxide (TOPO) and trioctylphosphine (TOP), that impart hydrophobicity to the QDs while inhibiting their aggregation in the solvent. However, to achieve effective PEC signals, it is necessary to establish electronic interactions between the surface of the QDs and specific biological species such as proteins, enzymes, and antigens. These interactions cannot be achieved in organic solvents and require an aqueous medium for their biological applications. The aqueous solubilization of QDs permits facile surface modification with biorecognition

elements such as antibodies, aptamers, and DNA for the transduction of photochemical signals. The surface functionalization of QDs is mainly achieved by three ways. The first approach is to synthesize the QDs using an aqueous synthetic route that involves the use of aqueous solvents and watersoluble ligands for stabilization of the QDs.<sup>38</sup> However, the aqueous synthetic route for soluble QD synthesis may not efficiently provide optimal optoelectronic properties, as the photophysical characteristics of QDs are highly prominent in the organic solvents.31 Ligand exchange of the hydrophobic moieties over the surface of the QDs for hydrophilic ones is another method for the aqueous solubilization of QDs. Most of the ligand exchange methods result in the surface modification of QDs with a variety of functionalities, such as -COOH, -NH<sub>2</sub> or -SH, at which biorecognition molecules can be anchored (Fig. 3b). 2,39,40 The third strategy consists of the hydrophilic encapsulation of QDs with different carrier vehicles such as amphiphilic polymers, silica coatings, and liposomes, which are among the most widely used encapsulation methods for the aqueous solubilization of QDs (Fig. 3b). 41-43

The attachment of biomolecules on the OD surface can be carried out by either non-covalent or covalent chemical reac-The covalent coupling of 1-ethyl-3-(3-dimethylaminopropyl)carbodiimide (EDC) and N-hydroxysuccinimide (NHS) activated carboxylate functional groups on QDs with those of the primary amine groups of biomolecules is one of the effective and rapid methods of QD bioconjugation. 44 Noncovalent binding can be accomplished by electrostatic, hydrophobic or high-affinity interactions between the surface of the QDs and the biomolecules. Although the electrostatic interactions involve simple affixation of the oppositely charged species without the use of crosslinking agents, it is rather weaker as compared with covalent conjugation. 45 High-affinity interactions consist of receptor-ligand, biotin-avidin/streptavidin, antigen-antibody and DNA interactions. Since these types of interaction may lead to large bioconjugates, EDC-coupled covalent interaction is the most commonly used approach for the bioconjugation of QDs in PEC-based sensing applications.46 QDs stabilized with aspartic acid and coated with polyethylene glycol (PEG) and a smaller sized tricysteine peptide sequence have been used as biolabels to selectively bind to polyhistidine-tagged (histag) proteins in in vitro settings and in living cells. These histag protein-QD complexes were applied to target individual proteins on the membrane of the living cells. 47,48 QDs modified with Tris-nitrilotriacetic acid (TrisNTA) (QD-TrisNTA) have been used to label polyhistidines on the cell-membranes of living cells (HeLa cells) expressing recombinant proteins. These QD-TrisNTA of different colors were used for orthogonal labeling to achieve multicolor tracking of proteins on living cells.<sup>49</sup> In another approach, hydrophilic dihydrolipoic acid-capped QDs (DHLA-QDs) were bioconjugated with polyhistidine peptides by a self-assembly process which is mediated by metal-affinity interactions. The polyhistidine peptide sequence on the DHLA-QDs allowed the dual functionality of binding to cellular membranes as well as intracellular labeling through their cellular internalization and

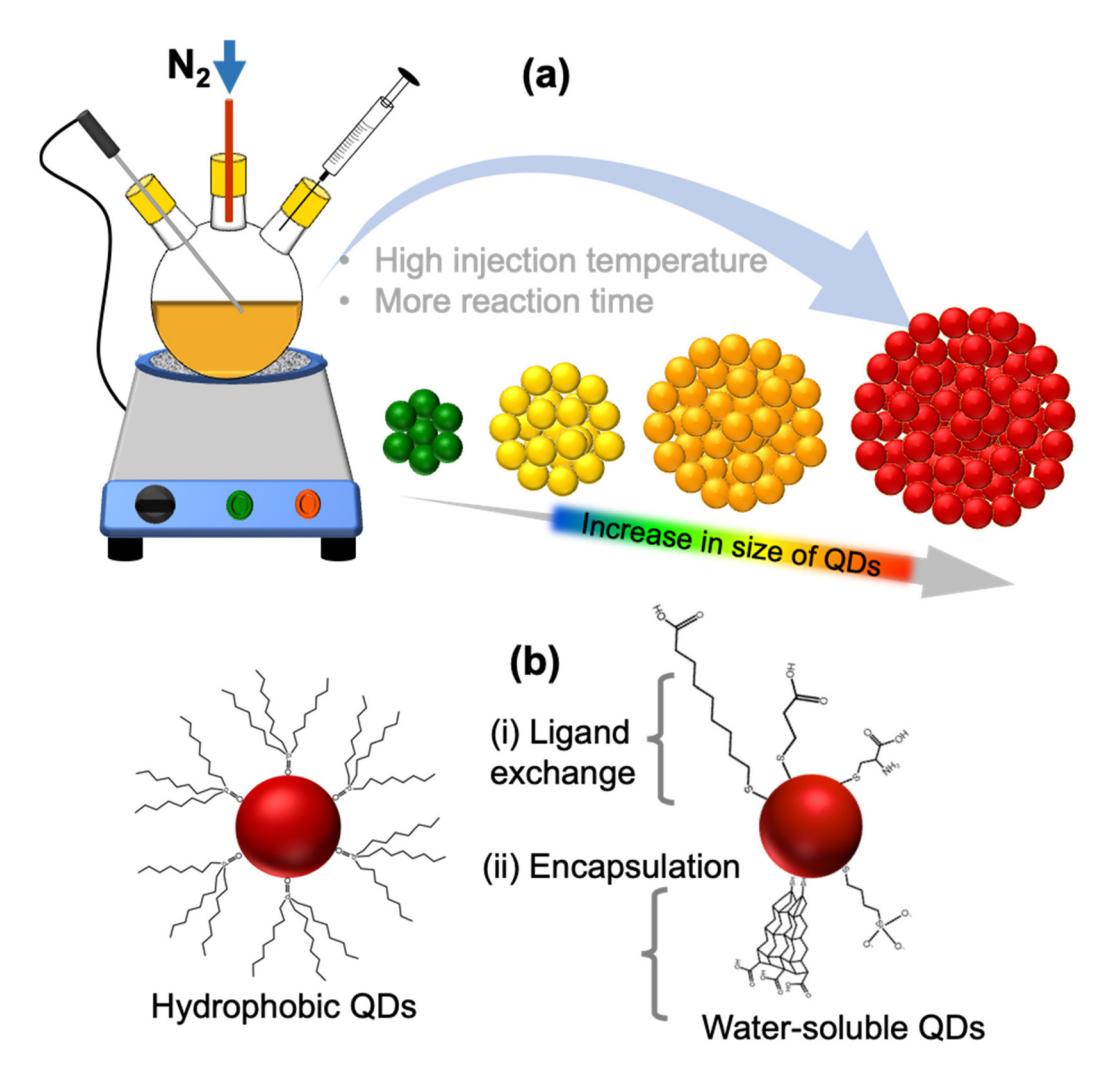


Fig. 3 (a) A typical setup for the synthesis of colloidal QDs, and (b) the schematic illustration of the procedure of surface modification of QDs showing: (i) ligand exchange of the hydrophobic ligands with water-soluble ones and (ii) encapsulation of hydrophobic QDs with hydrophilic polymers and silica coatings.

transmembrane delivery of QDs. The internalized QDs displayed a punctate-like staining pattern with partial QD signals being colocalized within the endosomes.<sup>50</sup> A number of other ligands binding at the QD surfaces have been excellently reviewed by Algar et al. 51 The developments in the design of QD-based bio-conjugates are not only applicable in bioassays, but also allow multi-colored tracking for the intracellular changes via their transmembrane delivery. In the following sections we discussed strategies applied for improving the photophysical properties of QDs that are essential in the realm of PEC sensing applications.

# Improving photophysical properties of QDs for PEC sensing

#### 4.1. Doping

Doping is the process of introducing impurities, known as dopants, into a semiconductor material in order to alter its

electrical properties. By adding an additional element to a nanocrystal, it is possible to tailor the bandgap of the semiconductor and introduce electronic states in the mid-gap region. Dopants can be either n-type, which provide extra electrons, or p-type, which provide extra holes, to the lattice.<sup>52</sup> This can affect the recombination and separation of charge carriers (electron-holes) in the nanocrystal structure, which can be exploited in applications such as photocurrent generation and sensing. For example, Mn2+ doping has been used to increase the photocurrent generation of CdS nanocrystals (QDs) and to develop sensors for hydrogen peroxide (H<sub>2</sub>O<sub>2</sub>) and glucose sensing. Mn2+ dopants in QDs that emit at 585 nm result in d-d transitions ( ${}^{4}T_{1} \rightarrow {}^{6}A_{1}$ ) in Mn<sup>2+</sup> with spin and orbital forbidden states as shown in Fig. 4(i). As a result, a lifetime of charge carriers (electron-hole pairs) is seen that is  $10^4$ – $10^5$  times (on the ms-scale) more than that of the undoped counterpart (on the ns-scale). The slowing of electron-hole recombination directly impacts the generation of the photocurrent. The phenomenon described above, in which

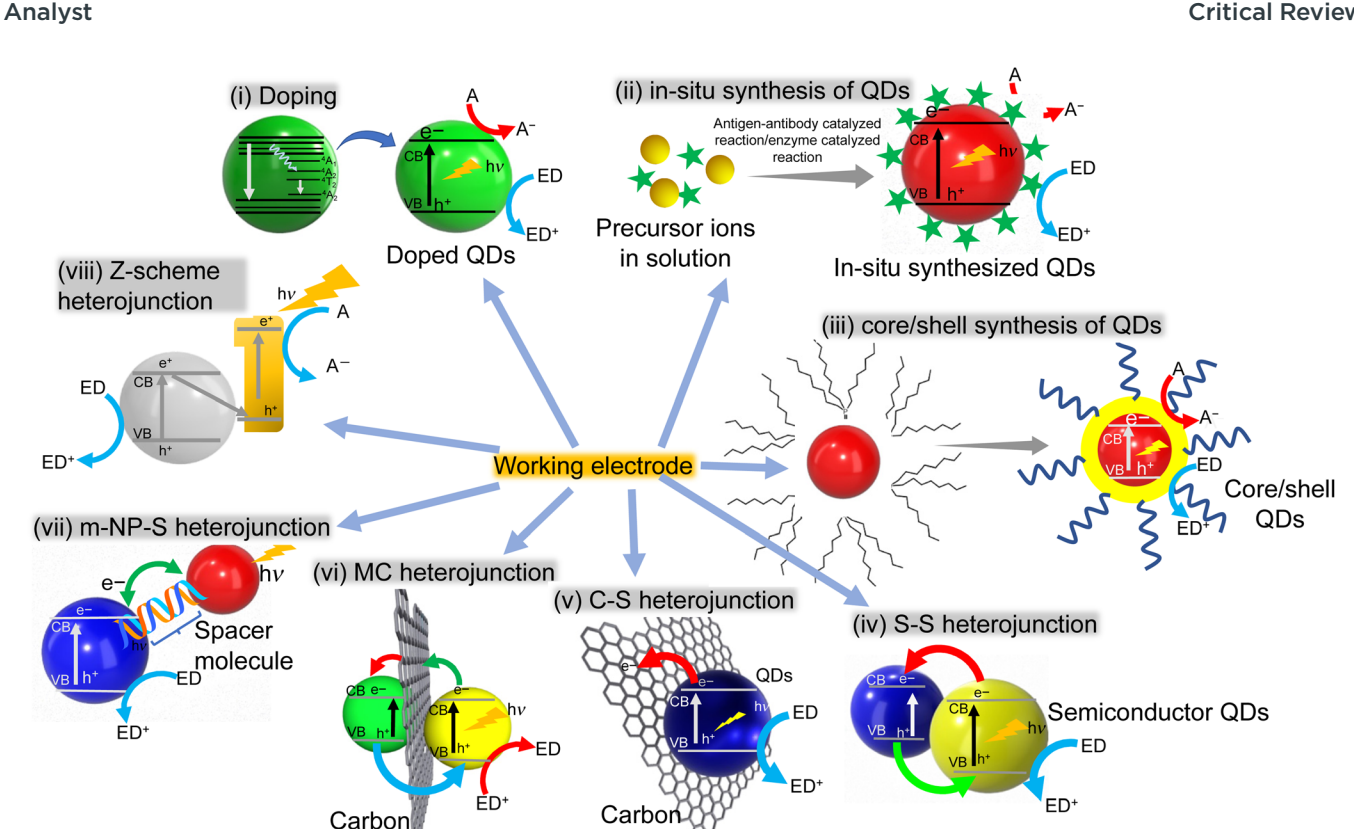


Fig. 4 A schematic illustration of various approaches used to improve the photophysical properties of semiconductor QDs in PEC biosensing applications: (i) doping of a semiconductor with another semiconductor that effects d-d transitions in a semiconductor and retards electron-hole recombination; (ii) in situ analyte molecule-induced synthesis of semiconductor QDs from precursor ions in solution; (iii) core/shell synthesis of semiconductor QDs; (iv) semiconductor-semiconductor (S-S) heterojunction; (v) carbon-semiconductor (CS) heterojunction; (vi) multicomponent (MC) heterojunction; (vii) metal nanoparticle-semiconductor (m-NP-S) heterojunction and (viii) Z-scheme heterojunction.

nanomaterial

dopants such as Mn<sup>2+</sup> can affect the recombination and separation of charge carriers (electron-holes) in a QD nanocrystal, has been utilized in various studies. For example, Tu et al. used Mn<sup>2+</sup> and Cu<sup>2+</sup> doped ZnSe QDs to develop a PEC sensor for detecting H<sub>2</sub>O<sub>2</sub> and glucose.<sup>53</sup> In this way, the unique properties of dopants and QDs can be exploited to develop sensitive and specific sensors for various analytes. Wu et al. found that the use of Mn<sup>2+</sup> dopants in CdS QD nanocrystals resulted in an 80% increase in photocurrent generation when used in the fabrication of a PEC cytosensor. 54 This demonstrates the potential of dopants to enhance the performance of PEC sensors through the improvement of sensitivity and signal amplification.

nanomaterial

#### 4.2. In situ synthesis of QDs

The immobilization of QDs on the surface of photoelectrodes is crucial for achieving enhanced PEC signals. One method for achieving this is using an in situ synthesis of QDs, which involves the direct participation of the analyte or the analytemediated formation of chemical species that favor the growth of QDs in solution. This can offer higher PEC sensing sensitivity due to the facile electron transfer kinetics in homogenous solutions, and also avoids the difficulties associated

with traditional surface modification processes (Fig. 4(ii)). 55,56 Enzymes such as horseradish peroxidase (HRP) can facilitate the in situ synthesis of QDs; for example, antibodies conjugated with HRP result in antigen-antibody complex formation while also releasing H2S as a result of the enzymatic reduction of sodium thiosulfate in the presence of H<sub>2</sub>O<sub>2</sub> substrate. The release of H<sub>2</sub>S during a chemical reaction can spontaneously react with cadmium ions (Cd<sup>2+</sup>) present in the same medium, leading to the in situ synthesis of QDs. These QDs can be observed as an enhanced photocurrent signal,23 and their in situ synthesis is a promising alternative approach for PEC sensing of bio-/chemical analytes.

#### Core-shell synthesis

An organic surfactant encapsulation strategy is generally applied to maintain the quantum confinement effect in QD. However, this type of encapsulation can lead to a decrease in the fluorescence quantum yield due to surface charge trap states, which contribute to the non-radiative de-excitation channels for charge carriers generated by photons. This issue can be addressed by synthesizing a core-shell QD structure, in which epitaxial gradient layers of inorganic material are grown over the core QD material. This can help to overcome the

reduction in fluorescence quantum yield caused by organic encapsulation. In core-shell QDs, a layer of an additional semiconductor material with a different bandgap than that of the core is typically formed at the periphery of the core QDs. This results in a substantial improvement in the photoluminescence efficiency of the ODs compared with those that are organic-encapsulated. The additional semiconductor layer at the periphery of the core QDs can help to reduce non-radiative de-excitation channels and increase the efficiency of the QDs (Fig. 4(iii)). In PEC sensing, passivating the core surface with an inorganic material that has a larger bandgap can help to inhibit the non-radiative recombination of excitons by reducing the number of non-radiative de-excitation channels and increase the efficiency of the PEC process.<sup>57</sup> This can be particularly useful for improving the accuracy and sensitivity of PEC sensors.

Riedel et al. developed a sarcosine sensor using core@shell (CdSe@ZnS) QDs immobilized on the surface of a Au electrode. In this system, the presence of a ZnS layer around the CdSe core prevented the formation of surface defects, which allowed for the generation of potential-dependent photocurrents upon illumination.<sup>58</sup> In an another study, a multibandgap engineered system was employed in which the core CdSeTe was first encapsulated by a CdS shell (sensitization shell), followed by a ZnS shell (passivating shell).<sup>59</sup> The presence of the CdS sensitization shell enhanced the ability to capture photons, and extend the lifetime of the electron-hole pair recombinations. On the other hand, the ZnS shell reduced the surface defect states and suppressed the electron recombination with external redox couples due to its wider bandgap, resulting in enhanced photocurrent generation. The bandgaps of the semiconductor layers in the CdSeTe/CdS/ZnS QDs were arranged in such a way that there was a gradual decrease in the potentials of the conduction bands starting from the CdSeTe core to the ZnS shell. The appropriate combination of semiconductor layers with properly aligned bandgap energies inhibits the recombination of charge carriers and thus enhances the photocurrent. The presence of a ZnS passivation shell inhibits the electron recombination with redox couples in solution and reduces the defect states and light corrosion with the CdSeTe@CdS QDs. This type of band alignment technique combines light-harvesting properties and enhances the lifetime of electron-hole pairs by inhibiting charge recombination.<sup>59</sup> Other PEC biosensors have been fabricated using similar core-shell QDs architectures, such as CdSe@ZnS, for the photoelectrochemical detection of amyloid β-protein.<sup>60</sup> The use of core-shell QDs in these sensors allowed for improved photoluminescence efficiency and sensitivity compared with other types of QD or sensing material.

#### 4.4. Formation of heterojunctions

To develop a high-sensitivity PEC sensor, it is necessary to improve the charge separation by properly arranging the QDs, semiconductor materials, and organic molecules on the surface of the sensor electrodes and fabricating different types of heterojunction. There are five strategies of which the first

four are commonly used for designing and fabricating heterojunctions for PEC sensing, which are discussed in the following sections. These strategies can help to optimize the efficiency and sensitivity of the PEC sensor by promoting effective charge separation and minimizing non-radiative deexcitation channels.

4.4.1 Semiconductor-semiconductor heterojunctions. Combining two semiconductors to form a heterojunction can facilitate the movement of charge from one semiconductor to another and promote efficient charge separation in PEC sensing. In this approach, semiconductor QDs can also be arranged with another semiconductor material or OD (Fig. 4 (iv)). One common strategy is to construct heterojunctions using metal oxides, such as TiO2, ZnO, WO3, SnO2 and NiO, with semiconductor QDs made up of elements such as CdS, CdSe, PbS, and MoS<sub>2</sub>. 5,61-63 In these cases, metal oxides typically have a larger bandgap than the incorporated core QDs, and this configuration has been used for the sensing of various analytes. For instance, Dai et al. fabricated a highly efficient PEC-based glucose sensor by using a 3D porous NiO nanolayer with a higher bandgap, which was integrated with PbS QDs on the surface of an ITO electrode. 64 In a heterojunction, two different semiconductor materials are brought into contact with each other, creating a junction between them. When these materials are irradiated with light, it can promote the transfer of electrons from the CB of one semiconductor to the CB of the other. At the same time, holes can be transferred from the VB of one semiconductor to the VB of the other. In other words, spontaneous transport of the photogenerated electrons takes place from the high-energy CB of one semiconductor to a lower-energy CB of another semiconductor, while at the same time, the holes travel from the lower-energy VB of one semiconductor material towards the higher-energy VB of the other semiconductor. This process can lead to an increased lifetime of charge carriers, as it produces the likelihood of electron-hole recombination, which can cause the carriers to disappear. In this way, the lifetime of charge carriers can be increased by efficiently inhibiting the process of electron and hole transfer recombination.5

4.4.2 Semiconductor-carbon heterojunctions. materials such as graphene, graphene oxide (GO), and singleand double-walled carbon nanotubes (CNTs) have been used to fabricate a semiconductor-carbon heterojunction as shown in Fig. 4(v). The formation of heterojunctions with carbon materials offers several advantages, such as higher electrical conductivity, thermal stability, high surface area and strong chemical and mechanical stability since a Schottky barrier function can be formed when a metal contacts with a semiconductor. This type of electrical junction can create a barrier that hinders the movement of charge carriers between the two materials. This barrier is formed due to the difference in energy levels between the metal's VB and the semiconductor's CB. The Schottky barrier can be used to inhibit the recombination of electrons and holes in a semiconductor device. By establishing a Schottky barrier between the semiconductor and another material, such as carbon, it can retard the recom**Analyst** Critical Review

bination process, leading to an increased lifetime of the charge carriers.

Carbon materials, such as graphene and CNTs, are known for their high electron mobility, which refers to the ability of electrons to move freely through the material. This property can be exploited in various applications. In the context of PEC sensing, carbon materials can be used to enhance the sensitivity and accuracy of the sensors. One way that carbon materials can be used in PEC sensing is by forming a heterojunction with a semiconductor material. By combining a carbon material with a semiconductor, it is possible to create a device that can efficiently absorb light and generate charge carriers. The high electron mobility of the carbon material can then promote the separation of charge carriers, leading to the enhanced PEC signal. In one example, GO and CdS QDs were combined to form a heterojunction for the PEC sensing of fumonisin. The energy levels of the VBs and CBs of the materials were carefully calculated to optimize the sensitivity of the sensor. 65 The combination of the high surface area of the GO and the light-absorption properties of the CdS QDs led to an enhanced PEC signal, enabling an accurate detection of fumonisin.65

Heterojunction devices composed of CdTe QDs with carbon materials have been shown to be effective for the PEC-based sensing of analytes. For example, a heterojunction composed of CdTe QDs and single-walled carbon nanohorns (SWCNHs) was used for the PEC sensing of streptomycin. The CdTe QDs and SWCNHs were synthesized through a one-pot synthetic protocol and deposited onto an ITO electrode. The aptamermediated restoration of the photocurrent was observed in the presence of streptomycin, indicating the sensitivity of the sensor to the drug. The function of SWCNHs in this device was to promote the signal amplification by inhibiting the charge recombination through fast electron transfer over their surface.66 In another example, a PEC sensor was fabricated using a composite of graphitic carbon nitride (g-C<sub>3</sub>N<sub>4</sub>) and CdS-QDs as the photoactive material for the sensitive detection of tetracycline. The overlapping bandgap energies of g-C<sub>3</sub>N<sub>4</sub> and CdS QDs allowed for effective light absorption and charge carrier generation, leading to a strong PEC signal in the presence of tetracycline. In another study, a highly efficient PEC electrode was fabricated using cationic water-soluble poly(allylamine hydrochloride)-modified graphene nanosheets (GNs-PAH) and the tailor-made negatively-charged CdS QDs.<sup>67</sup> GNs-PAH were used as nano-building-blocks for the sequential layer-by-layer (LbL) self-assembly of well-defined hybrid films of GNs-CdS QDs. The CdS QDs in the GNs-CdS are evenly spread over the 2D GNs on an FTO substrate. In this heterojunction, the CB of the CdS QDs is located above the work function of the GNs, indicating favorable charge transfer from the CB of the CdS QDs to the GNs upon visible light excitation. The photoexcited electrons captured by the GNs can be easily transferred to the FTO substrate, resulting in the separation of photogenerated electron-hole charge carriers and the production of photocurrent. Therefore, the integration of CdS QDs with GNs in an alternating manner and the 2D structural

advantage of GNs in GNs-CdS QDs composite films showed a significant enhancement in photoelectrochemical response and photocatalytic activity. Nong et al.68 fabricated an environmentally-friendly photoanode by embedding AgInS2 QDs into three-dimensional (3D) graphene nanowalls (GNWs). Here, AgInS<sub>2</sub> ODs with a tunable PL emission profile were fabricated by directly growing GNWs on silica, followed by the deposition of AgInS2 ODs. The interconnected GNWs 3D conductive network served as an excellent electron acceptor to transport the photogenerated carriers of AgInS2 QDs, resulting in a rapid photoresponse of AgInS2/GNW photoanodes upon light excitation. Other sensing heterojunction combinations, such as graphitic carbon nitride with CdS QDs<sup>69</sup> and graphene oxide with CdS QDs, 23 have also been used for the fabrication of PEC sensors.

4.4.3 Multi-component heterojunctions. Multi-component heterojunction devices are those in which two or more photoactive materials are arranged spatially with an electron transfer medium to provide efficient PEC activity. These types of system can be designed to take advantage of the unique properties of the different materials to enhance the PEC performance.

For example, a multi-component heterojunction composed of CdS, reduced graphene oxide (RGO), and ZnO nanowire arrays (NWAs) was fabricated for the PEC-based bioanalysis of glutathione. The heterostructure exhibited an enhanced PEC signal due to the synergistic effects of the high electron mobility of the ordered 1D ZnO NWAs, the extended visible-light absorption of the CdS nanocrystals, and the type II band alignment formed between them. The incorporated RGO showed excellent charge collection and shuttling characteristics, promoting the charge carrier separation and transfer process.70 Overall, multi-component heterojunctions with appropriate combinations of the photoactive materials can be useful for developing sensitive PEC sensor systems (Fig. 4(vi)). By carefully selecting the materials and optimizing the designs, it is possible to create highly efficient and sensitive PEC sensors for a variety of applications.

4.4.4. Metal nanoparticle-quantum dot hybrid heterojunctions. Modification of semiconductor QDs with plasmonic nanoparticles, such as Au, Ag and Pt nanoparticles, can enhance the light-harvesting properties of the PEC detection systems through the process of resonance energy transfer (RET). RET is an electrodynamic phenomenon in which nonradiative-energy transfer from energy-donor molecules to energy-acceptor molecules occurs through distance-dependent dipole-dipole interactions.71 The efficiency of this energy transfer is controlled by the distance (normally within 10 nm) and orientation of the donor and acceptor molecules, as well as the extent of spectral overlap between them.

There are two competing RET processes in PEC systems that are composed of plasmonic nanoparticles and semiconductor QDs, namely exciton energy transfer (EET) and plasmonic resonance energy transfer (PRET). EET tends to decrease photocurrents, while PRET increases them. Both processes can be exploited for the sensitive detection of analyte molecules in PEC biosensors.<sup>72</sup>

Semiconductor QDs generate excitons (electron-hole pairs) when exposed to light. These excitons can either recombine in a radiative and nonradiative manner, or result in the transfer of electrons to the surface of the electrode. When QDs and plasmonic nanoparticles are placed at a specific distance, exciton energy transfer (EET) from QDs to nanoparticles occurs through radiative or nonradiative routes, which can dampen the photocurrent signals.<sup>73</sup> On the other hand, metal nanoparticles exhibit surface plasmon resonance (SPR) once they interact with a specific wavelength of light in the visible to near-infrared range of the electromagnetic spectrum. The plasmonic nanoparticles convert the energy of incident photons to localized surface plasmon resonance (LSPR) and transfer the plasmonic energy to the proximity of semiconductor QDs, exciting more electron-hole pairs and thus enhancing the photocurrent. The transfer of energy from the plasmonic oscillation to the adjacent semiconductor promotes a higher concentration of carrier charges and improves the photocurrents. In addition, nonradiative decay can lead to the generation of electrons from the plasmon resonance that can be collected at the lower energy CB of the adjacent semiconductor, enhancing the photocurrent response. The integration of plasmonic nanostructures with QDs has gained attention due to its highly sensitive PEC-based sensing and analyte detection (Fig. 4(vii)). 5,73,74 As previously reported, when silver nanoparticles (Ag NPs) were linked with CdS QDs through DNA molecules, light irradiation activated the exciton-plasmon interactions (EPI), which was used to modulate the photocurrent generation from QDs. The generation of photocurrent can be tuned by adjusting the interparticle distance through EPI, leading to the sensitive detection of DNA.<sup>73</sup> The appropriate assembly of the photoactive semiconductor QDs with Au NPs has also been reported for the sensitive detection of E. coli bacterial cells, where the SPR-induced photogenerated charge enabled sensitive PEC sensing.<sup>75</sup>

4.4.5. Formation of Z-scheme heterojunctions. A photoactive heterojunction is an efficient system that produces electron-hole pairs through low-energy visible light-driven photoexcitation, which inhibits or delays the charge recombination event. The low-energy photons can only excite small bandgap semiconductors to create electron-hole pairs, while more negative conduction band and more positive valence band potentials are needed for a thermodynamically favorable redox reaction.<sup>76</sup> It can be challenging to meet these two conflicting conditions using traditional heterojunction fabrication methods, and therefore the recent development of a Z-scheme heterojunction has gained attention for its ability to efficiently separate electron-hole pairs from recombination. This type of heterojunction causes photoexcited electrons to travel through a Z-shaped pathway involving two photoactive materials with corresponding energy levels as shown in Fig. 4(viii). The Z-scheme heterojunction prevents electron-hole recombination and promotes high photocurrents with excellent redox capacity. The absorption of photons of a specific wavelength causes photoexcitation of the two materials (material I and II) to generate electron-hole pairs. Excited electrons in the CB of

material I move to the VB of material II at the interface and combine with the holes left in the VB of material II, producing a high photocurrent signal. The holes left in the VB of material I and the electrons left in the CB of material II can be easily consumed in forward oxidation and reduction reactions, respectively, eliminating any backward electron-hole recombination. 14

Recently, a Z-scheme heterojunction has been reported for the photoelectrochemical aptasensing of tetracycline using a CdTe QD and bismuth oxobromide (BiOBr) heterojunction. Under visible light illumination, the VB electrons in the CdTe and BiOBr are excited and promoted to the CB, respectively. Since the CB potential of CdTe QDs is more -ve than the reduction-potential of O<sub>2</sub>/O<sub>2</sub> and the VB potential of BiOBr is more +ve than the oxidation potential of H<sub>2</sub>O/OH, the photoelectrons from the CB of BiOBr follow a Z-scheme pathway that transfers them to the VB of the CdTe QDs. The proper alignment of electronic bandgaps between the materials forming the heterojunction leads to an efficient separation of the carrier charges, resulting in amplified photocurrent signals.<sup>77</sup> The Z-scheme heterojunction is a type of photoactive heterojunction that efficiently separates electron-hole pairs and promotes high photocurrents with excellent redox capacity, and it has been successfully used in PEC sensing. 78,79

## Applications of QDs in PEC-based biosensing

#### 5.1. Detection of disease biomarkers

There is a constant need to develop methods for the detection of disease biomarkers in order to better manage and treat relevant diseases. PEC sensors incorporating semiconductor QDs provide rapid, sensitive, and straightforward options for detecting certain disease biomarkers. Chen et al. presented a PEC sensing method for the detection of cardiac-troponin I (cTnI), a prominent predictive biomarker for cardiovascular diseases.80 In this work, a combination of a S-S heterojunction and metal nanoparticle-QD hybrid system was employed for the detection of cTnI. The hybrid system used CdS QD-sensitized TiO<sub>2</sub> nanosheets as a photoactive substrate, which were functionalized with a primary antibody (Ab<sub>1</sub>) specific to the cTnI biomarker protein, while a secondary antibody (Ab<sub>2</sub>) was labeled with Ag@Cu<sub>2</sub>O submicron particles composed of an Ag core with Cu2O shell (Ag@Cu2O SPs) for generating the signal (Fig. 5a). The immunoreaction that occurred in the presence of the cTnI antigen resulted in a decline in PEC signal due to a synergistic effect caused by the steric hindrance and high ascorbic acid (AA) consumption by the Ag@Cu2O SPs. The process for the photoelectrode fabrication and immunoreaction is illustrated in Fig. 5a and b. In this approach, Ag@Cu2O SPs are used as a photoactive material due to their strong light-harvesting properties and their ability to facilitate both RET and direct electron transfer (DET). The narrow bandgap p-type Cu<sub>2</sub>O semiconductor allows for a strong absorption of light, while the Ag core allows for RET and the injection of hot electrons at extended wavelengths (Fig. 5b).80

Ag@Cu₂O

Fig. 5 The schematic illustration of: (a) the surface functionalization of an  $ITO/TiO_2/CdS$  photoelectrochemical immunosensor sensor and sandwich assay with Ag@Cu<sub>2</sub>O submicron particles for the detection of cardiac troponin, and (b) a PEC sensor showing the electron transport mechanism from CdS-sensitized  $TiO_2$  nanohybrid and Ag@Cu<sub>2</sub>O SPs.<sup>80</sup> Reprinted with permission from ref. 80 (copyright © 2018 Elsevier B.V).

PEC sensing using Mn-doped CdS QDs and g-C<sub>3</sub>N<sub>4</sub> nanohybrids has been applied for detecting over-an expressed protein cancer biomarker, namely prostate-specific antigen (PSA), using a signal-off type of PEC biosensing strategy.<sup>81</sup> For effective PEC sensing, researchers fabricated a PEC electrode made of a nanohybrid of Mn-doped CdS QDs and functionalized with nano-graphitic carbon nitride (g-C<sub>3</sub>N<sub>4</sub>), and used it as a photoactive transducing element to generate the photocurrent signal (Fig. 6A). For signal amplification, a sandwich bioassay was designed based on concatamers of DNAzyme and hemin/G-quadruplex, which assisted the biocatalytic-precipitation on a fabricated CdS:Mn/g-C<sub>3</sub>N<sub>4</sub> photoelectrode (Fig. 6A and B). An immunocomplex is formed between: (i) a PSAcapture antibody (Ab1) that was immobilized on a fabricated PEC electrode, (ii) initiator strands, and (iii) antibody-conjugated AuNPs (So-AuNP-Ab2). Initiator strands with the immunocomplex trigger the hybridization-chain reaction between two DNA strands (DNA<sub>1</sub> and DNA<sub>2</sub>) to form a DNA concatemer. The addition of hemin molecules resulted in the formation of a DNAzyme, which precipitated in the presence of a 4-chloro 1-napthol compound. This reaction resulted in insulation of the PEC electrode that results in a decline in electron transfer at the electrode and hence leads to a decreased photocurrent. In this approach, the PSA level in the sample is determined by the formation of DNAzyme concatamers that biocatalyzed the precipitation of 4-chloro 1-napthol. PSA-dependent electrode surface insulation generated sensitive photocurrent signals with a PSA level as small as 3.8 pg mL<sup>-1</sup> (Fig. 6A).<sup>81</sup> Similarly, PSA detection has also been reported by other researchers utilizing QD-induced photoelectrochemical detection platforms.

The study reported by Cai et al.82 employed a unique sensing method utilizing EPI between a AuNP-graphene nanohybrid (AuNPs/GN) and a CdS QDs/TiO2 modified electrode. The surface of the CdS QDs/TiO2 electrode initially was conjugated with a capture DNA which allowed the AuNPs/GN-tagged PSA aptamer (receptor for PSA) to adhere via a hybridization-chain reaction between the aptamer-bases and capture-DNA. This arrangement causes a diminution in photocurrents through EPI between the CdS QDs and AuNPs. The quenching of photocurrents was found to be restored through a PSAmediated detachment of the AuNPs/GN from the electrode surface. The plasmon-exciton interaction between the AuNPs and CdS QDs allows the quenching of photocurrents, whereas the presence of PSA analyte captured by the aptamer displaces AuNPs/GN from the CdS QDs/TiO2 electrode surface, thus enhancing the photocurrent.82 The resonance-energy transfer between ZnCdHgSe QDs and Au nanorods was also studied to enhance PEC signals for the detection of PSA.<sup>72</sup>

#### 5.2. Detection of biomolecules

PEC-based detection techniques have been widely used to analyze biomolecules of clinical diagnostic concern, such as glucose, insulin and cholesterol. Both enzymatic and non-enzymatic approaches have been used to fabricate PEC sensors for these molecules. However, enzymatic sensors can have stability issues and require special storage and handling to protect them from environmental conditions. Non-enzymatic sensors, on the other hand, are more versatile and do not have these limitations.

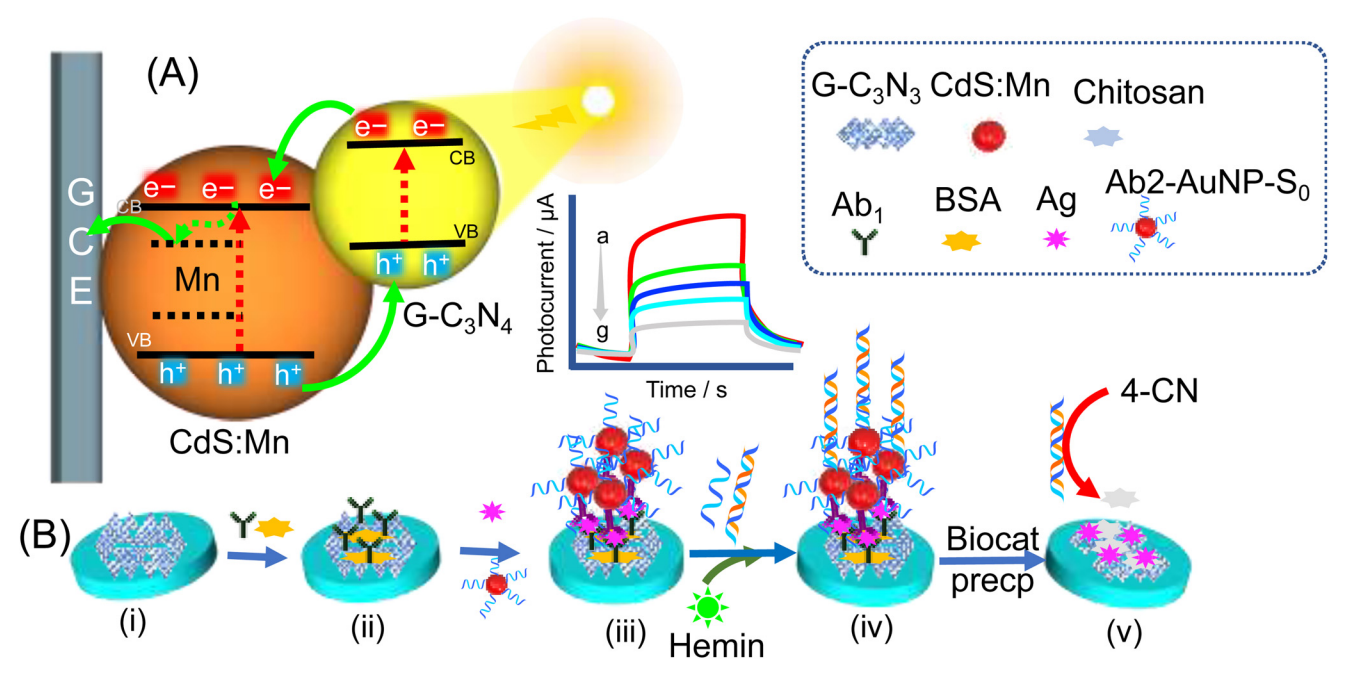


Fig. 6 The schematic illustration of: (A) mechanism of the generation of electron-hole pairs by Mn-doped CdS QDs and  $g-C_3N_4$  nanohybrids under light illumination, and biocatalyzed PSA-dependent insulation of the electrode surface. (B) Schematic illustration of the stepwise fabrication of the PEC sensing platform of: (i)  $g-C_3N_4/CdS:Mn/GCE$ ; (ii) sensor (i) +BSA/Ab<sub>1</sub>; (iii) sensor (ii) after reaction with PSA and  $S_0$ -AuNP-Ab<sub>2</sub>, and (iv) after the reaction with  $S_1$  and  $S_2$  + hemin, and (v) sensor (iv) +4-CN + H<sub>2</sub>O<sub>2</sub> (reprinted with permission from ref. 81, © 2017 Elsevier B.V.).

An efficient non-enzymatic sensor has been reported that consists of a graphene-CdS-nanohybrid as a carbon-semiconductor heterojunction for the direct PEC detection of glucose. The light illumination-generated electrons from the CB of the CdS move towards the CB of the ITO through highly conductive graphene nanosheets, while the OH<sup>-</sup> ions undergo oxidation to OH<sup>+</sup> by the photogenerated holes in alkaline solution that subsequently oxidizes glucose to gluconolactone that concomitantly generates the PEC signals (Fig. 7a and b). The process of photocurrent generation is schematically illustrated in Fig. 7a, c and d along with their responses recorded in Fig. 7b and e.<sup>83</sup>

Other enzymatic PEC glucose sensors based on QDs have also been reported by employing PbS-NiO and CdS-NiO as photoactive materials in PEC electrodes. 64,84 Wang, G.-L. et al. 84 reported an enzymatic PEC glucose sensor using a CdS QD-sensitized 3D nanoporous NiO photocathode (Fig. 7c-e). Though CdS is a typical n-type narrow bandgap semiconductor capable of generating anodic photocurrent itself, the sensitization of it with the larger bandgap p-type semiconductor NiO leads to the switching of the charge transfer direction of the electrode. Moreover, coupling of the two semiconductors, namely CdS and NiO, changes the PEC response from the UV range to the visible light range (Fig. 7c and d). The photogenerated holes from the electron-hole pair in the CdS move towards the VB of the NiO and the holes in the NiO were neutralized by the supply of electrons from the ITO electrode, and this produces a cathodic photocurrent. Since the VB potential of the CdS is more positive compared with the VB potential of the NiO, a hole-driving gradient promotes the effective transfer of holes from the CdS to the NiO, facilitating an efficient charge separation. The presence of dissolved  $\rm O_2$  in the medium serves as an electron acceptor for the photogenerated electrons in the CdS and produces a stable photocurrent (Fig. 7e). Moreover, the assembly of the glucose oxidase (GOx) recognition enzyme, layer-by-layer over the surface of the CdS-NiO/ITO electrode, and the introduction of different concentrations of glucose to the photoelectrochemical system, triggered the enzymatic oxidation of the glucose, which subsequently depleted the dissolved oxygen and generated a corresponding decrease in photocurrents.  $^{84}$ 

In a similar approach, glucose sensing was carried using glucose oxidase immobilized on a PbS QD-NiO/ITO electrode. Here, the cathodic photocurrent was observed due to the movement of holes from the PbS to the NiO layer and the subsequent transfer of electrons from the electrode to scavenge holes in the NiO layer. Moreover, the photogenerated electrons in the PbS were captured by the dissolved oxygen in the electrolytic solution, promoting electron-hole separation (Fig. 8a). The enzymatic oxidation of glucose through GOx causes a depleted oxygen supply, which resulted in a photocurrent reduction, and the concentration of glucose was directly proportional to the decrease in the photocurrent response using this PEC sensor (Fig. 8b).<sup>64</sup>

Recently, Ma J. et al.<sup>85</sup> reported a glucose sensor based on an enzyme-linked photoelectrochemical assay. The PEC response of the sensor was modulated to absorb visible light.

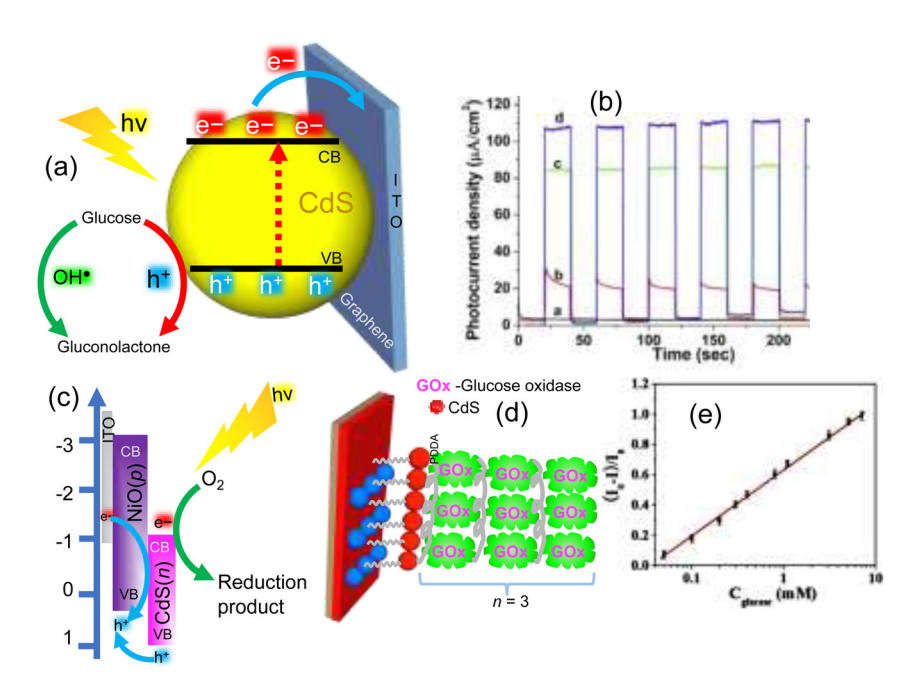


Fig. 7 (a) Schematic illustration showing photocurrent generation with photoelectrode graphene-CdS/ITO, and (b) photocurrent responses for the detection of glucose<sup>83</sup> (a and b reprinted with permission from ref. 83, Copyright © 2014 Elsevier Ltd). Schematic diagram showing: (c) energy band alignment of CdS QDs and NiO, (d) assembly of GOx at the surface of the electrode made of CdS QDs-NiO/ITO, and (e) the linear photocurrent response generated from the photoelectrode (GOx/CdS QDs-NiO/ITO) against varying concentrations of glucose<sup>84</sup> (c–e Reprinted with permission from ref. 84, Copyright © 2014 Elsevier B.V.).

In this approach, the photoactive electrode material was constructed using a nanocomposite composed of nanorods/QDs made of TiO<sub>2</sub>/polydopamine (PDA)/glucose oxidase through hydrothermal synthesis and subsequent photopolymerization. After a proper arrangement of TiO2 QDs between the TiO2 NRs and the PDA, an effective heterojunction was formed that not only facilitated effective electron transport across the electrode, but also improved the response by the modified-electrode toward the visible light (Fig. 8e). PDA undergoes  $\pi$ - $\pi$  electronic transitions upon its excitation by visible light. Therefore, the excited electrons in the PDA move, starting from the highest occupied molecular orbital (HOMO) to the lowest unoccupied molecular orbital (LUMO). These photoexcited electrons travel to the CB of the QDs, and then to the CB of the TiO<sub>2</sub>, which is attributed to the proper alignment with decreasing CB band potentials, making the electrons channeled to the FTO electrode. Moreover, the photogenerated holes in the PDA travel to the GOx enzyme that facilitated the oxidation of the glucose. The dependence of the photocurrent on the concentration of glucose was found to be linear in the range of 0-4 mM, allowing accurate glucose sensing (Fig. 8d).85

Another biologically important analyte that has been detected using PEC is a neurotransmitter called [2-(3,4-dihydroxyphenly)ethylamine] or dopamine, which is a neurotransmitter that plays a key role in the central nervous system, and also serves as a hormone and has a variety of effects on regulating metabolic and cardiovascular systems. Recently, a few attempts have been made toward the development of PEC-based sensors for detecting dopamine. In PEC platforms for

such analytes, typically electrons-holes are generated upon illumination and these carriers are subsequently captured by oxidative and reductive species to generate a photocurrent. Wang et al. 7 constructed a unique PEC biosensor for the detection of dopamine. In this study, dopamine is oxidized to polydopamine that acts as an efficient electron acceptor and captures photogenerated electrons from the CdS QDs. Fig. 8e depicts a model for this photoelectrochemical process. During a photoelectrochemical event, the presence of electron donors, such as triethanolamine (TEA), shows stable anodic photocurrents with a CdS QD-modified ITO electrode by neutralizing the photogenerated holes. When dopamine was added to a solution, it undergoes oxidization to form a polymer called polydopamine. This can occur under mild alkaline conditions or through electrodeposition in a neutral Polydopamine contains benzoquinone groups, which act as electron scavengers. When it is present in a solution containing CdS QDs, the benzoquinone groups can scavenge the photogenerated electrons in the CdS QDs, reducing the photocurrent. This reduction in photocurrent can be used to detect the presence of dopamine, manifested as a decreased photocurrent signal (Fig. 8f).<sup>7</sup>

A DNA-detecting PEC sensor has been reported that utilizes a Z-scheme assembly of the overlapping electronic bands of CdSe QDs and amino-functionalized graphene QDs. The primary layer was fabricated with reduced graphene oxide and CdTe QDs that exhibited anodic photocurrent signals. The resulting electrode comprised ITO/PDDA-rGO/CdSe QDs, which was later subjected to a T-DNA-dependent catalytic

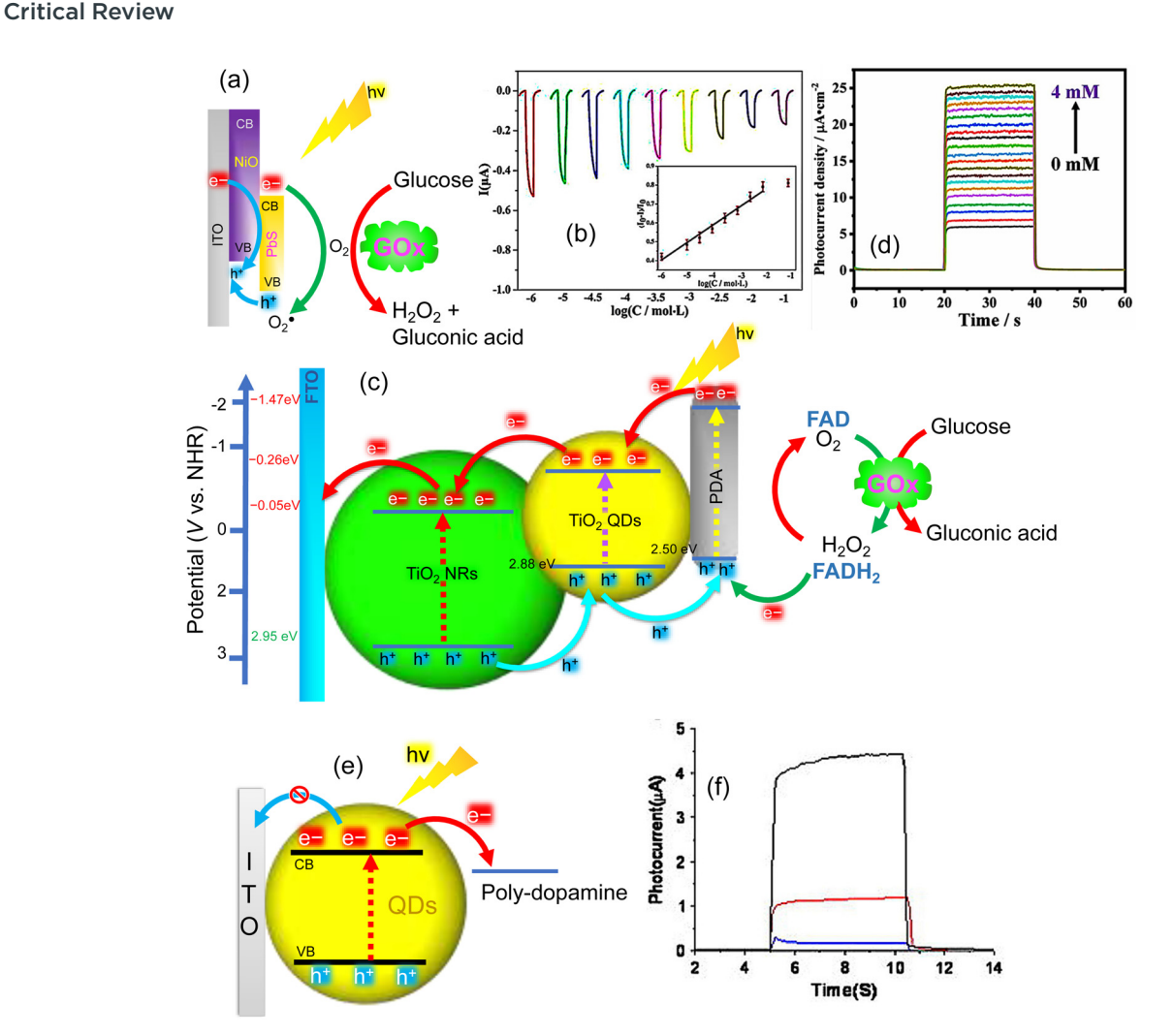


Fig. 8 (a) Schematic illustration showing the photoelectrochemical oxidation of glucose at a GOx-immobilized PbS-NiO/ITO electrode, and (b) the PEC response from the GOx-immobilized PbS-NiO/ITO electrode against varying glucose concentrations in mM.<sup>64</sup> (a and b reprinted with permission from ref. 64 Copyright © 2017, American Chemical Society.) (c) Schematic illustration showing the mechanism of PEC sensing of glucose at a glucose oxidase/PDA/TiO2 QDs/TiO2 NRs/FTO photoelectrode along with different band potentials in eV, and (d) the sensor photocurrent response in the presence of varying glucose concentrations<sup>85</sup> (c and d reprinted with permission from ref. 85 Copyright © 2022, American Chemical Society). (e) Schematic illustration showing the mechanism of electron transfer at the electrode (CdS QDs/ITO) in the presence of polydopamine, and (f) changes in the photocurrent responses of the QDs (CdS) modified ITO electrode in the absence (black line) and in the presence of polydopamine through oxidation of alkaline solution (red line) and electrodeposition (blue-line)<sup>7</sup> (e and f reprinted with permission from ref. 7 Copyright © 2014 Elsevier B.V.).

hairpin-assembly, and chain reaction hybridization that led to the formation of abundant long-strand DNA molecules on the sensor platform (Fig. 9(a)). The incubation of these DNA molecules on the sensing platform containing amino-functionalized graphene QDs led to a Z-scheme PEC sensing system, which switches the photoelectrochemical anodic current to the cathodic current. This type of current setup was demonstrated for DNA-dependent enhanced photoelectrochemical signals with zero background current as shown in Fig. 9(b). The current scheme offers an efficient method for the sensing of T-DNA with negative background signals and a linear calibration plot was achieved in the range of 1 aM-100 pM of DNA between the logarithmic concentration of DNA and the photocurrent signals (Fig. 9c).87

#### 5.3. Analysis of drugs

Semiconductor QD-based PEC detection systems can also be employed for the analysis of certain antibiotics and antiinflammatory drugs. An aptasensor has been reported by Okoth, O. K. et al. for the sensitive detection of diclofenac (an anti-inflammatory drug) utilizing the carbon-semiconductor heterojunction conjugated with Au NPs.74 Here, a graphenedoped CdS QDs (GR-CdS QDs) modified FTO electrode was used as a photoactive platform with incorporated Au NPs and exhibited an increase in photocurrent response due to surface plasmon resonance. In this case, Au NPs were beneficial for immobilizing the thiol-functionalized diclofenac (DCF) aptamer with its terminal -SH group, and the immobilized

(a) CdSe QDs dsDNA Cationic polymer coated rGO Capture probe (CP) 1 **AGQDs** cathode CdSe QDs (ii) anode Time Alkane thiol Target **AGQDs** CPs-2 (b) (c) 20 20 Photocurrent / μΑ Photocurrent / µA

Fig. 9 (a) Schematic illustration of DNA-associated Z-scheme CdSe QDs/AGQDs CdSe for the PEC sensing of T-DNA, (b) photocurrent signals generated by the PEC sensor against varying T-DNA concentrations, such as 0, 0.1 aM to 10 nM (shown with an arrow from  $a \rightarrow 0$ ) and (c) plot showing the relationship between the photocurrent value and the T-DNA analyte concentration. The inset shows the linearity for varying concentrations (fM) against the photocurrent in terms of μA.87 (a-c reprinted with permission from ref. 87 copyright © 2019 Elsevier B.V.)

Light-off

aptamer acted as a biorecognition element. DCF molecules were then captured by the aptasensor once the immobilized aptamers came into contact with DCF in the medium. When visible light was illuminated on the sensor, the oxidation of captured DCF took place due to the photogenerated holes, and as a result, an enhanced PEC current response was realized (Fig. 10a).<sup>74</sup> This sensor exhibited a linear PEC response against the concentration range of 1-150 nM DCF, with a limit of detection (3S/N) of 0.78 nM under optimized conditions.

10

Light-on

In another report, CdTe QDs coated with single-walled carbon nanohorns (CdTe-SWCNHs) were utilized in fabrication of PEC aptamer sensor and used for detecting the antibiotic drug called streptomycin.88 The CdTe-SWNH nanocomposite was synthesized via a one-pot protocol, and this nanocomposite was used to modify the surface of an ITO electrode (Fig. 10b). Upon irradiation, a noticeable cathodic photocurrent was observed due to the presence of SWCNHs that promoted a fast electron transfer by the inhibition of charge

recombination. However, a decrease in photocurrent intensity was observed when the surface of the CdTe-SWCNHs/ITO electrode was conjugated with streptomycin aptamer ligands, resulting in a steric effect caused by the aptamer molecules (Fig. 10b). In the presence of streptomycin, the aptamer was stripped off from the electrode and restored the photocurrent, as shown in Fig. 10b. The intensity of the photocurrent, under optimized conditions, is directly proportional to the streptomycin concentration in the range of 0.1-50 nM with a limit of detection = 0.33 nM (Fig. 10c).88

ż logc / fM

#### 5.4. Detection of pathogens

PEC sensing has also been applied for the fast and robust detection of microorganisms, such as bacterial cells. Yang et al.89 fabricated a high-performance PEC sensor using a unique strategy for the detection of sulfate-reducing bacteria. Sulfate-reducing bacteria actively secrete secondary metabolites, for instance H<sub>2</sub>S, and the presence of metal ions pro-

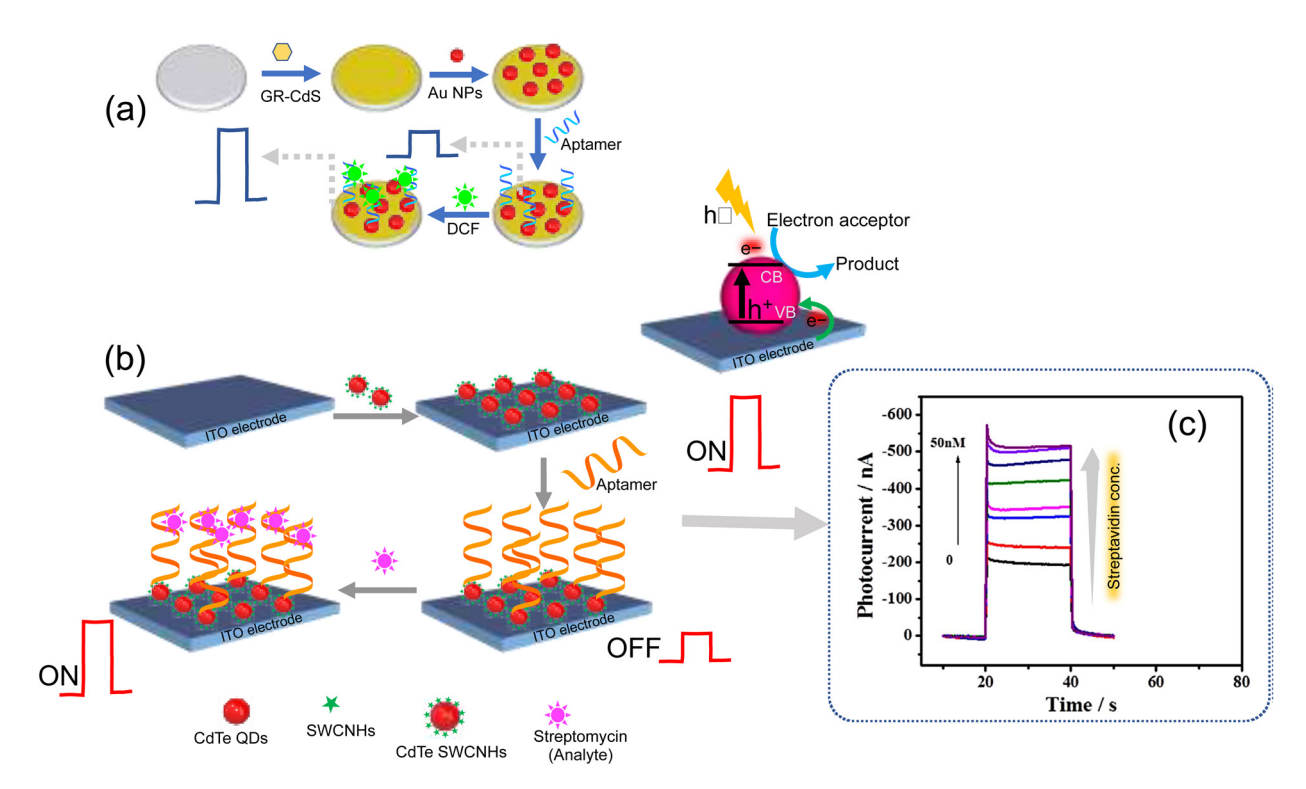


Fig. 10 (a) Schematic illustration of Au/GR-CdS photoelectrode preparation and functionalization of Au/Ps modified with aptamer ligand on a PEC electrode. The photocurrent responses of the sequential modification of electrodes with bare FTO, GR-CdS, Au/GR-CdS, aptamer-Au/GR-CdS and DCF aptamer-Au/GR-CdS in 0.1 M Na<sub>2</sub>SO<sub>4</sub> at 0.2 V of applied potential<sup>74</sup> (a reprinted with permission from ref. 74 copyright © 2018 Elsevier B.V.). (b) Scheme showing the aptamer-based photoelectrochemical process at a CdTe-SWCNH-modified ITO electrode, (c) photoelectrochemical responses of an ssDNA-based aptasensor against 0.1 nM to 50 nM concentrations of streptomycin at the CdTe-SWCNH-modified ITO electrode<sup>88</sup> (b and c reprinted with permission from ref. 88 copyright © 2017 Published by Elsevier B.V.).

motes their nucleation to form nanoparticles. This phenomenon has been exploited, where a semiconductor-semiconductor heterojunction is established due to the in situ generation of H2S, which mediated the growth of CdS QDs over the ZnO nanorod arrays in the presence of the externally added Cd<sup>2+</sup> ions. Therefore, the amount of CdS QD production mediated the enhancement of photocurrent that corresponded to the bacterial cell numbers and concomitant generation of metabolic H<sub>2</sub>S (Fig. 11a and b).<sup>89</sup> In the above PEC-based sensing approach, the in situ synthesis of QDs can be triggered by the other secondary metabolites, similar to H2S that could provide a highly effective and sensitive means for detecting living bacteria, as well as tracking metabolic reactions in the cells, which remains to be explored.

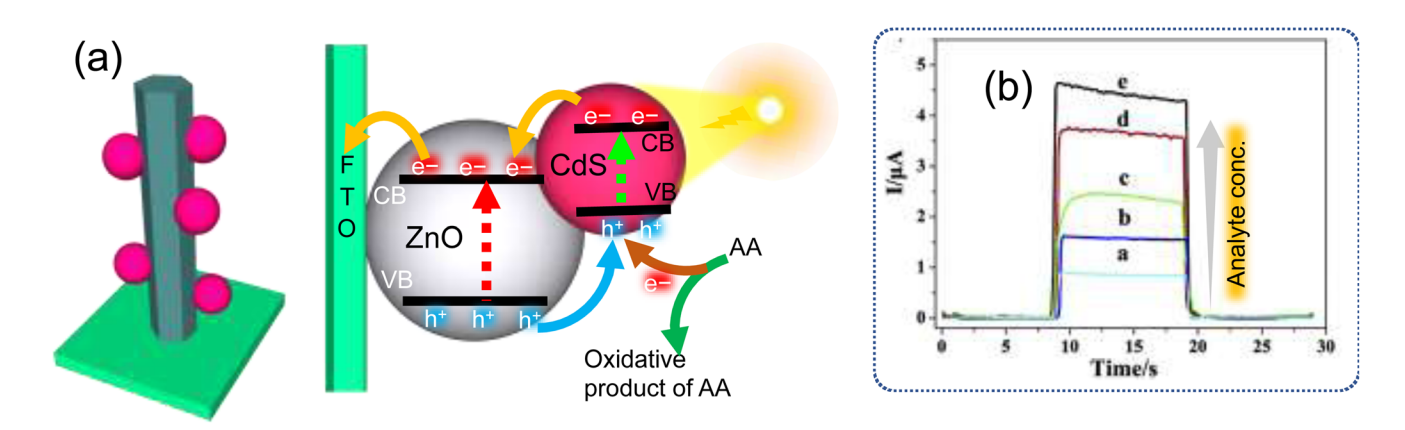


Fig. 11 (a) Schematic illustration for the PEC sensing mechanism and (b) photocurrent for different concentrations of sulfate-reducing bacteria (SRB) ( $a-e = 10^2 - 10^6$  colony forming units per mL, respectively) at the fabricated CdS QDs/ZnO nanorod array-modified fluorine-doped tin oxide (FTO) electrode of the PEC sensor.<sup>89</sup> (a and b reprinted with permission from ref. 89 copyright © 2018 Published by Elsevier B.V.)

 Table 1
 A list of notable semiconductor QD-based PEC sensing attempts made for the detection of biomolecules, metabolites and pathogens that have been tested, electrode-modifying materials used and experimental conditions are presented in the table

Calcille trapeoin   Aggictic obdoctd-sob, TOOITO   O. IM PES + 0.12 MAA   Son W.Elbimp   Son W	Target analyte	Heterojunction/electrode	Buffer	Light source	Time (s)	Applied potential (V)	Ref.
Authorson	Biomarkers Cardiac troponin 1 (Prostate-specific antigen)	Cu <sub>2</sub> O-Ab <sub>2</sub> /CdS-Ab <sub>1</sub> /TiO/ITO INPs-Ab <sub>2</sub> /Ab <sub>1</sub> /g-C <sub>3</sub> N <sub>4</sub> /CdS:Mi	0.1 M PBS + 0.12 M AA 0.1 M PBS + 0.1 M KCl	100 W LED lamp 500 W Xe lamp	16	0.6	80
PATRONEON CASES   PATRONES AND CASE   PATRONES AND CASE	PSA PSA	GCE AuNPs-GN-PSA aptamer/CdS-TiO <sub>2</sub> -	0.1 M PBS pH 7.4 + 0.001 M AA	500 W 200–2500 nm	10 on/	0	73
Parametric Care Cache	PSA Cellular H <sub>2</sub> S Carcinoembryonic antigen	DNAFTO Anti PSA-AuNRs-ZnCdHgSe/GCE B-TiO-CdS/FTO AgNCs-GRNCs-Ab <sub>2</sub> /Ab <sub>1</sub> -CdS:Mn/TiO <sub>2</sub> /	0.1 M PBS pH 7 + 0.2 M AA 0.01 M PBS pH 7.4 + 0.1 M AA 0.1 M PBS pH 7.4 + 0.1 M AA	5 W Solar light 500 W xenon lamp	ПО	0 0	72 55 90
Example         Aptramer-AutNPs/GR-CdS/FTO         0.1 M Na <sub>3</sub> SO <sub>4</sub> Xe lamp 420 nm         Xe lamp 420 nm           olocules         Aptramer-CdTe-SWCNHs/ITO         0.1 M PBS PH 5.5         Misble light source 468 nm         Aptramer 468 nm           olocules         PAPAGENTAD         0.1 M PBS PH 5.5         200 W xeroon lamp 420 nm         100 W LED lamp 430 nm           see         GAR-CdS/ITO         0.1 M PBS PH 7         100 W LED lamp 430 nm         100 W LED lamp 430 nm           see         GAR-CdS/ITO         0.1 M Tris-HCl buffer pH 7.0         5 W light-emitting diode lamp 430 nm         100 ml           see         GAVCdS/NIO/ITO         0.1 M Tris-HCl buffer pH 7.0         5 W light-emitting diode lamp 430 nm         100 ml           see         GAVCdS/NIO         0.1 M Tris-HCl buffer pH 7         400 nm         100 ml           mine         DAA/CdS/ITO         0.1 M Tris-HCl buffer pH 7.4 + 0.1 M AA         400 nm         10 on/           sine         cdsegZnS/CdS/ITO         10 mM Tris-HCl buffer pH 7.4 + 0.1 M AA         420 nm         10 on/           sine         CdSegZnS/GS/ITO         10 mM Tris-HCl buffer pH 7.4 + 0.1 M AA         420 nm         10 on/           sine         CdS/ITO/CdT-c/cdS/M TriO-y/ITO         11 m Tris-HCl buffer pH 7.4 + 0.1 M AA         300 W         10 on/           <	(CEA) CEA IL-6	F1O In situ produced CdS on GO/ITO CdSe-LL6/Ab-CdS/TiO/ITO	0.1 M Tris-HCl buffer pH 7.4 + 0.1 M AA 0.1 M PBS pH 7.4 + 0.1 M AA	480 nm 405 nm 500 W 200–2500 nm	10 on 10 off	-0.2 0	23
Deba@CNT-Ab_/PDA-Ab_/CdS/WO <sub>2</sub> 0.1 M PBS pH 7         180 W LED lamp 430 nm           See         Gox/PbS/NiO/ITO         0.1 M Tris-HCl buffer pH 7.0         5 W light-emitting diode         10 on/           See         Gox/PbS/NiO/ITO         0.1 M Tris-HCl buffer pH 7.0         5 W light-emitting diode         10 on/           see         Gox/CdS/NIO/ITO         0.1 M Tris-HCl buffer pH 7.0         0.0 W Xe lamp         10 on/           mine         ZnIn <sub>2</sub> S <sub>4</sub> /CdS/ITO         10 mM Tris-HCl buffer pH 7.4         490-500 nm         0ff           mine         PDA/CdS/ITO         0.1 M FBS pH 9 + 0.1 M TEA         490-500 nm         0ff           n stinc         PDA/CdS/ITO         0.1 M PBS pH 7.4 + 0.1 M AA         490-500 nm         10 on/           sine         CdSc@ZnONS/Ola         10 mM Tris-HCl buffer pH 7.4 + 0.1 M AA         420 nm         10 on/           sine         CdSc@ZnONBS/FTO         0.1 M PBS PH 7.4 + 0.1 M AA         350 mW         0ff           sgens         CdS/ZnONBS/FTO         0.1 M PBS PH 7.4 + 0.1 M AA         350 mm         10 on/           richia coli 0157:H7         FTO         0.1 M PBS PH 7.4 + 0.1 M AA         455 mm         10 off           sins         Aun PBS PH 7.4 + 0.1 M AA         350 W Xe lamp 410 mm         10 off	Drugs Diclofenac Streptomycin Tetracycline Dicarologados	Aptamer-AuNPs/GR-CdS/FTO Aptamer-CdTe-SWCNHs/ITO Aptamer/g-C <sub>3</sub> N <sub>4</sub> -CdS/FTO	$0.1  \mathrm{M  Na_2 SO_4} \\ 0.1  \mathrm{M  PBS  pH  5.5} \\ 0.1  \mathrm{M  Na_2 SO_4}$	Xe lamp 420 nm Visible light source 468 nm 300 W xenon lamp 420 nm		0.2 0 +0.4	74 88 69
See         Gav-Cds/ITOD         0.1 M NaOH         and High-temitting diode         10 on/ lamp 415 nm         off           See         Gox/Cds/NiO/ITO         0.1 M Tris-HCl buffer pH 7.0         0.1 M Tris-HCl buffer pH 7.0         10 w Xe lamp         off           see         Gox/Cds/NiO/ITO         0.1 M Tris-HCl buffer pH 8.5 + 0.05 mM Trs         490-500 nm         off           mine         PDA/Cds/ITO         0.1 M PBS pH 9 + 0.1 M Trs         490-500 nm         10 on/           nice         I cholinesterase AChE         In situ-produced CdS QDs/ITO         0.1 M PBS pH 9 + 0.1 M Trs         10 on/           sine         CdSe@Zns-SoOAu         HEPES buffer pH 7.4 + 0.1 M AA         230 nm         10 on/           sine         AGQDs/DNA/CdSe QDs/PDDA-rGO/         0.1 M Tris-HCl buffer pH 7.4 + 0.1 M AA         420 nm         10 on/           gens         I ro         10 mM Tris-HCl buffer pH 7.4 + 0.1 M AA         420 nm         10 on/           gens         AGS/ZnONRs/FTO         0.1 M PBS pH 7.4 + 0.1 M AA         500 W         10 on/           re-reducing bacteria         CdS/ZnONRs/FTO         0.1 M PBS pH 7.4 + 0.1 M AA         Xe lamp 350 nm         10 on/           sine         AGO/CdS/ITO         0.1 M PBS pH 7.4 + 0.1 M AA         455 nm         10 on/           sine <td< td=""><td>Insulin</td><td>PDA@CNT-Ab<sub>2</sub>/PDA-Ab<sub>1</sub>/CdS/WO<sub>3</sub>/</td><td>0.1 M PBS pH 7</td><td>180 W LED lamp 430 nm</td><td></td><td>0</td><td>61</td></td<>	Insulin	PDA@CNT-Ab <sub>2</sub> /PDA-Ab <sub>1</sub> /CdS/WO <sub>3</sub> /	0.1 M PBS pH 7	180 W LED lamp 430 nm		0	61
see         GOX/CdS/NIO/ITO         0.1 M Tris-HCl buffer pH 7         in ph 415 mm         OIT           mine         2nIn <sub>2</sub> S <sub>4</sub> /CdS/ITO         (triethanolamine)         10 mM Tris-HCl buffer pH 8.5 + 0.05 mM TreA         400 nm         10 m           mine         pDA/CdS/ITO         0.1 M PBS pH 9 + 0.1 M TrA         490-500 nm         10 on/V           1 cholinesterase AChE         in situ-produced CdS QDs/ITO         pBS 0.1 M pH 7.4 + 0.1 M AA         430 nm         10 on/V           1 cdc-CdTe/CdS/Gans-SO/Au         HEBPES buffer pH 7.4 + 0.1 M AA         230 mW         10 on/V         0ff           AGQDs/DNA/CdSe QDs/IDOA         0.1 M Tris-HCl buffer pH 7.4 + 0.1 M AA         420 nm         10 on/V         0ff           Irreteducing bacteria         cds/ZnONRs/FTO         0.1 M PBS pH 7 + 0.01 M AA         500 W         10 on/V           Introducing bacteria         cdsQDs@aptamerAuNPs/ZnONWs/         0.01 M PBS pH 7.4 + 0.1 M AA         Xe lamp 350 nm         10 on/V           Ainsin B1         GO/CdS/ITO         0.1 M PBS pH 7.4 + 0.1 M AA         455 nm         200 nm           AuNPs-DNA/CdS-NH <sub>2</sub> -DNA/ITO         0.1 M PBS pH 7.4 + 0.1 M AA         500 W Xe lamp 410 nm         10 off	Glucose Glucose	ITO GR-CdS/ITO Gox/PbS/NiO/ITO	0.1 M NaOH 0.1 M Tris-HCl buffer pH 7.0	5 W light-emitting diode	10 on/	0 0	83
mine         ZnIn <sub>2</sub> S <sub>4</sub> /CdS/ITO         10 mM Tris-HCl buffer pH 8.5 + 0.05 mM TEA         400 nm           mine         PDA/CdS/ITO         0.1 M PBS pH 9 + 0.1 M TEA         490-500 nm           sine         CdSe@ZnS-SO/Au         PBS 0.1 M PH 7.4 + 0.1 M AA         430 nm         10 on/Om           sine         CdSe@ZnS-SO/Au         HEPES buffer pH 7.6         230 mW         0ff           cdTe/CdTe/CdS:Mn/TiO <sub>2</sub> /ITO         0.1 M Tris-HCl buffer pH 7.4 + 0.1 M AA         420 nm         10 on/Off           sgens         AGQDs/DNA/CdSe QDs/PDDA-rGO/         10 mM Tris-HCl buffer pH 7.4 + 0.1 M AA         420 nm         10 on/Off           per-educing bacteria         CdS/ZnONRs/FTO         0.1 M PBS pH 7 + 0.01 M AA         500 W         10 on/Off           re-reducing bacteria         CdS/ZnONRs/FTO         0.1 M PBS + 0.1 M AA         Xe lamp 350 nm         20 on           virinia SI         GO/CdS/ITO         0.1 M PBS PH 7.4 + 0.1 M AA         455 nm         20 on           AuNPs-DNA/ITO         0.1 M PBS PH 7.4 + 0.1 M AA         550 W W ke lamp 410 nm         10 off	Glucose	GOx/CdS/NiO/ITO	0.1 M Tris-HCl buffer pH 7	samp 415 nm 500 W Xe lamp	ПО	0	84
PDA/CdS/ITO   PDA/CdS/ITO   PBS pH 9 + 0.1 M TEA   500 W   5	Dopamine	ZnIn <sub>2</sub> S <sub>4</sub> /CdS/ITO	10 mM Tris-HCl buffer pH 8.5 + 0.05 mM TEA (triethanolamine)	400 nm 10 W		0	92
CdSe@ZnS-SO/Au   HEPES buffer pH 7.4 + 0.1 M AA   430 nm   10 on off off off off off off off off off	Dopamine	PDA/CdS/ITO	0.1 M PBS pH 9 + 0.1 M TEA	490–500 nm 500 W		0	^
gens         AGQDS/DNA/CdSe QDS/PDDA-rGO/         10 mM Tris-HCl buffer pH 7.4 + 0.1 M AA         420 mm         10 on/           gens         AGQDS/DNA/CdSe QDS/PDDA-rGO/         10 mM Tris-HCl buffer pH 7.4 + 0.1 M AA         420 mm         10 on/           re-reducing bacteria         CdS/ZnONRs/FTO         0.1 M PBS pH 7 + 0.01 M AA         Xe lamp 350 mm         10 on/           vrichia coli O157:H7         CdSQDS@aptamerAuNPs/ZnONWs/         0.01 M PBS pH 7.4 + 0.04 M AA         Xe lamp 350 mm         20 on           vins         Auns         GO/CdS/TTO         0.1 M PBS pH 7.4 + 0.04 M AA         455 mm         20 on           AunPs-DNA/CdS-NH <sub>2</sub> -DNA/ITO         0.1 M PBS pH 7.4 + 0.1 M AA         500 W Xe lamp 410 mm         10 off	Acetyl cholinesterase AChE Sarcosine	<i>In situ</i> -produced CdS QDs/ITO CdSe@ZnS-SO/Au	PBS 0.1 M pH 7.4 + 0.1 M AA HEPES buffer pH 7.6	400 mm 430 mm 230 mW	10 on 10 on/	0 -0.35	56 58
ogens         AGQDS/DNA/CdSe QDS/PDDA-rGO/         10 mM Tris-HCl buffer pH 7.4 + 0.1 M AA         420 mm         10 m/           re-reducing bacteria         CdS/ZnONRs/FTO         0.1 M PBS pH 7 + 0.01 M AA         500 W         10 m/           rrichia coli O157:H7         CdSQDs@aptamerAuNPs/ZnONWs/FTO         0.01 M PBS + 0.1 M AA         Xe lamp 350 nm         20 on           xins         AunRs-DNA/TTO         0.1 M PBS pH 7.4 + 0.0 M AA         455 nm         20 on           AunPs-DNA/CdS-NH2-DNA/TTO         0.1 M PBS pH 7.4 + 0.1 M AA         500 W Xe lamp 410 nm         10 off	DNA	CdTe/CdTe/CdS:Mn/TiO <sub>2</sub> /ITO	$0.1~\mathrm{M}$ Tris-HCl buffer pH $7.4+0.1~\mathrm{M}$ AA		оп 10 on/	0	83
gens     Oct Mode Service     Oct Mode Describing Des	DNA	AGQDs/DNA/CdSe QDs/PDDA-rGO/ ITO	10 mM Tris-HCl buffer pH 7.4 + 0.1 M AA	420 nm	on 10 on/ off	-0.1 V	87
richia coli O157:H7         CdSQDs@aptamerAuNPs/ZnONWs/ FTO         0.01 M PBS + 0.1 M AA         Xe lamp 350 nm           xins         GO/CdS/TTO         0.1 M PBS pH 7.4 + 0.04 M AA         455 nm         20 on 10 off           AuNPs-DNA/CdS-NH <sub>2</sub> -DNA/ITO         0.1 M PBS pH 7.4 + 0.1 M AA         500 W Xe lamp 410 nm	Pathogens Sulfate-reducing bacteria	CdS/ZnONRs/FTO	0.1 M PBS pH 7 + 0.01 M AA	500 W		0	88
	(SKB) Escherichia coli O157:H7	CdSQDs@aptamerAuNPs/ZnONWs/ FTO	0.01 M PBS + 0.1 M AA	Xe lamp 350 nm		0	75
10 OH AUNPS-DNA/CdS-NH <sub>2</sub> -DNA/ITO 0.1 M PBS pH 7.4 + 0.1 M AA 500 W Xe lamp 410 nm	<b>Biotoxins</b> Fumonisin B1	GO/CdS/ITO	0.1 M PBS pH 7.4 + 0.04 M AA	455 nm	20 on		65
	${ m Hg}^{2+}$	AuNPs-DNA/CdS-NH <sub>2</sub> -DNA/ITO	0.1 M PBS pH 7.4 + 0.1 M AA	500 W Xe lamp 410 nm	110 011	0	93

PEC sensors with both light-harvesting and charge separation property capabilities of the embedded QDs can prove to be effective tools for remotely detecting pathogenic microorganisms, or for combating disease outbreaks in remote and resource-limited locations. Only a few attempts have been made toward utilizing the above feature since the last decade. For instance, an efficient PEC sensor composed of ZnO nanowires (ZnO NWs), Au NPs and CdS QDs is utilized for the detection of the pathogenic bacterium Escherichia coli. The surface of a PEC sensor electrode consisted of ZnO NWs and Au NPs that were functionalized with receptor aptamer-coated CdS QDs. In this PEC system, the choice and alignment of the photoactive surfaces played a significant role and therefore the CdS QDs/AuNPs/ZnO NW assembly offered effective charge separation due to an efficient band alignment of the semiconductors, as well as rapid charge transfer through the Au NPs. The attachment of E. coli cells over the CdS QDs@aptamer influenced the photocurrent to linearly decrease with a proportionally increasing concentration of E. coli cells.<sup>75</sup>

Various PEC sensors based on QD-interfaced heterojunction photoelectrodes have been developed for detecting bioanalytes, such as biomolecules/biomarkers, metabolites, and pathogens (Table 1). The fabrication of QD interfaced PEC sensors has been extended for biosensing applications mainly for disease biomarker detection, such as cardiac troponin 1, PSA, CEA, IL-6, glucose, and DNA molecules. A few researchers focused on the development of QD-based PEC heterojunctions, in combination with metal/metal oxide nanoparticles, for pathogenic bacteria detection. Also, PEC QDs with carbon nanomaterial heterojunction electrodes were fabricated, which were functionalized with a specific aptamer receptor for the detection of drug molecules.

Despite the advancement in the QD-based PEC sensor electrode fabrication strategies, there remain still several challenges that need to be addressed. For instance, the cost and scalable fabrication of PEC sensor electrodes depends on the substrate, such as ITO and FTO, and miniaturization, flexibility and self-powered functioning become vital for their exploitation. One of these challenges can be addressed by utilizing a flexible polymeric substrate onto which ITO nanoparticles can be directly grown. Another challenge is related to proper arrangement of the bandgap in QDs with metal/metal oxide and/or graphene/CNTs for the fabrication of PEC electrodes. A well-designed heterojunction using appropriate functional nanomaterials and charge transport layers can facilitate efficient electron transport across the electrode, which improves the response of the modified electrode.

#### Conclusions

PEC sensing has gained significant attention due its ability to detect a wide range of chemical species and biomolecules with a high sensitivity and fast response. QDs are particularly useful in PEC sensing due to their ability to absorb a wide range of wavelengths of light and their narrow emission

spectra, which allows for the design of simple, inexpensive, miniaturized, and portable PEC sensor platforms. The facile surface properties of QDs make them suitable for efficient chemical coupling with biomolecules and other moieties, enabling the detection of a wide range of biomolecules that cannot be detected using conventional optical methods. Overall, the use of QDs in PEC sensing offers many advantages, making them a promising technology for a variety of analytical and medical diagnostic applications.

This review summarizes recent progress in the design and fabrication of QD-interfaced PEC sensors, including their use in the detection of disease biomarkers, biomolecules, drugs, pathogens, and other chemical/biological species. PEC sensors involve the use of a light source to excite the photoactive material and generate a photoelectrical current as an output signal. The mechanism of PEC sensing relies on the separation and excitation of charge carriers, which allows for high sensitivity with minimal background signal. Various designs of QDs-interfaced heterojunction strategies have been proposed to enhance the photoelectric conversion efficiency in PEC sensing. However, the design and fabrication of QD-interfaced PEC sensors for biosensing applications is still in its infancy and faces several challenges, including the limited-use Cdbased QDs, the need for environmentally friendly QDs, and the lack of in situ synthetic approaches for interfacing QDs directly in the vicinity of the PEC electrode. These challenges must be addressed in order to promote the practical use of QD-interfaced PEC sensors. In order to make QD-based PEC sensors more practical for biosensing applications, it is important to consider the use of biocompatible semiconductor QDs, such as InP, SnSe, and CuInSe2 with tunable bandgap energies, in the design and fabrication of heterojunction materials. However, the synthesis of environmentally friendly QDs is still a challenge due to the use of toxic solvents and expensive precursor salts. Most PEC sensors, however, rely on the use of externally synthesized colloidal QDs. A notable and effective PEC sensing method involved the synthesis of QDs in situ, and directly in the vicinity of the electrode, which is triggered by the presence of an analyte. This type of in situ QDs synthesis is mediated by enzymatic catalysis, such as by horseradish peroxidase (HRP) and the precursor ions, H<sub>2</sub>O<sub>2</sub> and H<sub>2</sub>S. The reaction allows for the detection of analyte through the simultaneous nucleation of QDs at the PEC electrode, which is governed by the presence of the analyte.

Designing and fabricating PEC sensors as flexible, simple, and miniaturized wearable devices could be beneficial for biosensing and biomedical applications, particularly in the field of wearable technology. These sensors could be powered by solar cells or self-powered systems, making them low cost and portable. Wearable PEC sensors have the potential to revolutionize personalized and preventive healthcare technology.

#### Conflicts of interest

There are no conflicts to declare.

Analyst Critical Review

### Acknowledgements

This work was supported by the TÜBİTAK 1004 NANOSİS, project no. 20AG004 and the authors are grateful for this support.

#### References

- 1 R. Keçili, S. Büyüktiryaki and C. M. Hussain, *Trends Anal. Chem.*, 2019, **110**, 259–276.
- 2 A. Tufani, A. Qureshi and J. H. Niazi, *Mater. Sci. Eng., C*, 2021, **118**, 111545.
- 3 M. Mahmoudpour, J. E. N. Dolatabadi, M. Torbati and H.-R. Aziz, *Biosens. Bioelectron.*, 2019, 127, 72–84.
- 4 E. N. Özmen, E. Kartal, M. B. Turan, A. Yazıcıoğlu, J. H. Niazi and A. Qureshi, *Mater. Sci. Eng.*, C, 2021, 129, 112356.
- 5 J. Shu and D. Tang, Anal. Chem., 2019, 92, 363-377.
- 6 Z. Rong, Z. Bai, J. Li, H. Tang, T. Shen, Q. Wang, C. Wang, R. Xiao and S. Wang, *Biosens. Bioelectron.*, 2019, **145**, 111719.
- 7 G.-L. Wang, H.-J. Jiao, K.-L. Liu, X.-M. Wu, Y.-M. Dong, Z.-J. Li and C. Zhang, *Electrochem. Commun.*, 2014, 41, 47– 50.
- 8 Z.-X. Zhang and C.-Z. Zhao, *Chin. J. Anal. Chem.*, 2013, 41, 436–444.
- 9 D. Dong, D. Zheng, F.-Q. Wang, X.-Q. Yang, N. Wang, Y.-G. Li, L.-H. Guo and J. Cheng, *Anal. Chem.*, 2004, 76, 499–501.
- 10 N. Haddour, J. Chauvin, C. Gondran and S. Cosnier, J. Am. Chem. Soc., 2006, 128, 9693–9698.
- 11 Y. Zang, J. Fan, Y. Ju, H. Xue and H. Pang, *Chem. Eur. J.*, 2018, 24, 14010–14027.
- 12 J. Wang, W. Lv, J. Wu, H. Li and F. Li, *Anal. Chem.*, 2019, **91**, 13831–13837.
- 13 A. Ikeda, M. Nakasu, S. Ogasawara, H. Nakanishi, M. Nakamura and J.-i. Kikuchi, *Org. Lett.*, 2009, 11, 1163– 1166
- 14 L. Yang, S. Zhang, X. Liu, Y. Tang, Y. Zhou and D. K. Y. Wong, *J. Mater. Chem. B*, 2020, **8**, 7880–7893.
- 15 W.-W. Zhao, J.-J. Xu and H.-Y. Chen, *Trends Anal. Chem.*, 2016, **82**, 307–315.
- 16 E. Golub, G. Pelossof, R. Freeman, H. Zhang and I. Willner, Anal. Chem., 2009, 81, 9291–9298.
- 17 X. Zhang, S. Li, X. Jin and X. Li, *Biosens. Bioelectron.*, 2011, **26**, 3674–3678.
- 18 A. Devadoss, P. Sudhagar, C. Terashima, K. Nakata and A. Fujishima, *J. Photochem. Photobiol.*, *C*, 2015, **24**, 43–63.
- 19 Z. Yue, F. Lisdat, W. J. Parak, S. G. Hickey, L. Tu, N. Sabir, D. Dorfs and N. C. Bigall, ACS Appl. Mater. Interfaces, 2013, 5, 2800–2814.
- 20 D. Geißler and N. Hildebrandt, *Anal. Bioanal. Chem.*, 2016, **408**, 4475–4483.
- 21 W. W. Tu, Z. Y. Wang and Z. H. Dai, *TrAC, Trends Anal. Chem.*, 2018, **105**, 470–483.

- 22 N. Hildebrandt, C. M. Spillmann, W. R. Algar, T. Pons, M. H. Stewart, E. Oh, K. Susumu, S. A. Díaz, J. B. Delehanty and I. L. Medintz, *Chem. Rev.*, 2017, 117, 536–711.
- 23 X. Zeng, W. Tu, J. Li, J. Bao and Z. Dai, ACS Appl. Mater. Interfaces, 2014, 6, 16197–16203.
- 24 W.-W. Zhao, M. Xiong, X.-R. Li, J.-J. Xu and H.-Y. Chen, *Electrochem. Commun.*, 2014, 38, 40–43.
- 25 Q. Liu, Y. Yin, N. Hao, J. Qian, L. Li, T. You, H. Mao and K. Wang, *Sens. Actuators B Chem.*, 2018, **260**, 1034–1042.
- 26 L. Shi, Y. Yin, L.-C. Zhang, S. Wang, M. Sillanpää and H. Sun, *Appl. Catal.*, *B*, 2019, 248, 405–422.
- 27 N. Tomczak, R. Liu and J. G. Vancso, *Nanoscale*, 2013, 5, 12018–12032.
- 28 J. Cassidy and M. Zamkov, J. Chem. Phys., 2020, 152, 110902.
- 29 D. Sumanth Kumar, B. Jai Kumar and H. M. Mahesh, in *Synthesis of Inorganic Nanomaterials*, ed. S. Mohan Bhagyaraj, O. S. Oluwafemi, N. Kalarikkal and S. Thomas, Woodhead Publishing, 2018, pp. 59–88, DOI: 10.1016/B978-0-08-101975-7.00003-8.
- 30 F. Divsar, Quantum Dots, in Quantum Dots—Fundamental and Applications; IntechOpen: London, UK., 2020, DOI: DOI: 10.5772/intechopen.83206.
- 31 R. Gill, M. Zayats and I. Willner, *Angew. Chem., Int. Ed.*, 2008, 47, 7602–7625.
- 32 Y. Zang, J. Fan, Y. Ju, H. Xue and H. Pang, *Chem. Eur. J.*, 2018, **24**, 14010–14027.
- 33 R. Freeman, R. Gill, M. Beissenhirtz and I. Willner, *Photochem. Photobiol. Sci.*, 2007, **6**, 416–422.
- 34 U. Badıllı, F. Mollarasouli, N. K. Bakirhan, Y. Ozkan and S. A. Ozkan, *Trends Anal. Chem.*, 2020, 116013.
- 35 A. Qureshi, A. Tufani, G. Corapcioglu and J. H. Niazi, *Sens. Actuators B Chem.*, 2020, **321**, 128431.
- 36 M. F. Frasco and N. Chaniotakis, *Sensors*, 2009, **9**, 7266–7286.
- 37 A. M. Smith, G. Ruan, M. N. Rhyner and S. Nie, *Ann. Biomed. Eng.*, 2006, **34**, 3–14.
- 38 N. Gaponik and A. L. Rogach, in *Semiconductor Nanocrystal Quantum Dots*, Springer, 2008, pp. 73–99.
- 39 B.-K. Pong, B. L. Trout and J.-Y. Lee, *Langmuir*, 2008, 24, 5270–5276.
- 40 J. Aldana, N. Lavelle, Y. Wang and X. Peng, *J. Am. Chem. Soc.*, 2005, **127**, 2496–2504.
- 41 T. Wang, R. Sridhar, A. Korotcov, A. H. Ting, K. Francis, J. Mitchell and P. C. Wang, *Colloids Surf.*, A, 2011, 375, 147–155.
- 42 N. Beloglazova, P. Shmelin, E. Speranskaya, B. Lucas, C. Helmbrecht, D. Knopp, R. Niessner, S. De Saeger and I. Y. Goryacheva, *Anal. Chem.*, 2013, 85, 7197–7204.
- 43 N. Beloglazova, O. Goryacheva, E. Speranskaya, T. Aubert, P. Shmelin, V. Kurbangaleev, I. Y. Goryacheva and S. De Saeger, *Talanta*, 2015, 134, 120–125.
- 44 K. E. Sapsford, T. Pons, I. L. Medintz and H. Mattoussi, *Sensors*, 2006, **6**, 925–953.
- 45 R. Bilan, F. Fleury, I. Nabiev and A. Sukhanova, *Bioconjugate Chem.*, 2015, **26**, 609–624.

46 I. Martynenko, A. Litvin, F. Purcell-Milton, A. Baranov,

A. Fedorov and Y. Gun'Ko, J. Mater. Chem. B, 2017, 5, 6701-

Critical Review

- 47 C. M. Green, D. Mathur, K. Susumu, E. Oh, I. L. Medintz and S. A. Díaz, in Bioluminescence: Methods and Protocols, ed. S.-B. Kim, Springer US, New York, NY, 2022, vol. 2, pp. 61-91, DOI: 10.1007/978-1-0716-2473-9\_6.
- 48 A. Dif, F. Boulmedais, M. Pinot, V. Roullier, M. Baudy-Floc'h, F. M. Coquelle, S. Clarke, P. Neveu, F. Vignaux, R. L. Borgne, M. Dahan, Z. Gueroui and V. Marchi-Artzner, J. Am. Chem. Soc., 2009, 131, 14738-14746.
- 49 V. Roullier, S. Clarke, C. You, F. Pinaud, G. Gouzer, D. Schaible, V. Marchi-Artzner, J. Piehler and M. Dahan, Nano Lett., 2009, 9, 1228-1234.
- 50 J. B. Delehanty, I. L. Medintz, T. Pons, F. M. Brunel, P. E. Dawson and H. Mattoussi, Bioconjugate Chem., 2006, 17, 920-927.
- 51 W. R. Algar, K. Susumu, J. B. Delehanty and I. L. Medintz, Anal. Chem., 2011, 83, 8826-8837.
- 52 R. Buonsanti and D. J. Milliron, Chem. Mater., 2013, 25, 1305-1317.
- 53 L. Tu, G. Liu, W. Zhang, J. Qin and Z. Yue, IEEE J. Sel. Top. Quantum Electron., 2014, 20, 175-183.
- 54 P. Wu, J. B. Pan, X. L. Li, X. Hou, J. J. Xu and H. Y. Chen, Chem. - Eur. J., 2015, 21, 5129-5135.
- 55 Y. Wang, S. Ge, L. Zhang, J. Yu, M. Yan and J. Huang, Biosens. Bioelectron., 2017, 89, 859-865.
- 56 T. Hou, L. Zhang, X. Sun and F. Li, Biosens. Bioelectron., 2016, 75, 359-364.
- 57 W.-W. Zhao, X.-D. Yu, J.-J. Xu and H.-Y. Chen, Nanoscale, 2016, 8, 17407-17414.
- 58 M. Riedel, G. Göbel, A. M. Abdelmonem, W. J. Parak and F. Lisdat, ChemPhysChem, 2013, 14, 2338-2342.
- 59 S. Zhou, Y. Wang, M. Zhao, L. P. Jiang and J. J. Zhu, ChemPhysChem, 2015, 16, 2826-2835.
- 60 J. Feng, F. Li, X. Li, X. Ren, D. Fan, D. Wu, H. Ma, B. Du, N. Zhang and Q. Wei, J. Mater. Chem. B, 2019, 7, 1142-1148.
- 61 R. Wang, H. Ma, Y. Zhang, Q. Wang, Z. Yang, B. Du, D. Wu and Q. Wei, Biosens. Bioelectron., 2017, 96, 345-350.
- 62 B. Zhang, H. Wang, H. Ye, B. Xu, F. Zhao and B. Zeng, Sens. Actuators B Chem., 2018, 273, 1435-1441.
- 63 A. Qileng, S. Yang, J. Wei, N. Lu, H. Lei, Y. Liu and W. Liu, Sens. Actuators B Chem., 2018, 267, 216-223.
- 64 W.-X. Dai, L. Zhang, W.-W. Zhao, X.-D. Yu, J.-J. Xu and H.-Y. Chen, Anal. Chem., 2017, 89, 8070-8078.
- 65 L. Mao, K. Ji, L. Yao, X. Xue, W. Wen, X. Zhang and S. Wang, Biosens. Bioelectron., 2019, 127, 57-63.
- 66 X. Xu, D. Liu, L. Luo, L. Li, K. Wang and T. You, Sens. Actuators B Chem., 2017, 251, 564-571.
- 67 F.-X. Xiao, J. Miao and B. Liu, J. Am. Chem. Soc., 2014, 136, 1559-1569.
- 68 J. Nong, G. Lan, W. Jin, P. Luo, C. Guo, X. Tang, Z. Zang and W. Wei, J. Mater. Chem. C, 2019, 7, 9830-9839.

- 69 Y. Liu, K. Yan and J. Zhang, ACS Appl. Mater. Interfaces, 2016, 8, 28255-28264.
- 70 K. Zhao, X. Yan, Y. Gu, Z. Kang, Z. Bai, S. Cao, Y. Liu, X. Zhang and Y. Zhang, Small, 2016, 12, 245-251.
- 71 Y. Chu, T. Han, A. Deng, L. Li and J.-J. Zhu, Trends Anal. Chem., 2020, 123, 115745.
- 72 Y. Wang, X. Yu, X. Ye, K. Wu, T. Wu and C. Li, Anal. Chim. Acta, 2016, 943, 106-113.
- 73 W.-W. Zhao, P.-P. Yu, Y. Shan, J. Wang, J.-J. Xu and H.-Y. Chen, Anal. Chem., 2012, 84, 5892-5897.
- 74 O. K. Okoth, K. Yan, J. Feng and J. Zhang, Sens. Actuators B Chem., 2018, 256, 334-341.
- 75 X. Dong, Z. Shi, C. Xu, C. Yang, F. Chen, M. Lei, J. Wang and Q. Cui, Biosens. Bioelectron., 2020, 149, 111843.
- 76 P. Zhou, J. Yu and M. Jaroniec, Adv. Mater., 2014, 26, 4920-4935.
- 77 Z. Guo, K. Jiang, H. Jiang, H. Zhang, Q. Liu and T. You, J. Hazard. Mater., 2022, 424, 127498.
- 78 X. Chen, W. Wu, Q. Zhang, C. Wang, Y. Fan, H. Wu and Z. Zhang, Biosens. Bioelectron., 2022, 114523.
- 79 R. Xu, K. Xu, Y. Du, J. Li, X. Ren, H. Ma, D. Wu, Y. Li and Q. Wei, Anal. Chem., 2022, 9888-9893.
- 80 J. Chen, L. Kong, X. Sun, J. Feng, Z. Chen, D. Fan and Q. Wei, Biosens. Bioelectron., 2018, 117, 340-346.
- 81 K. Zhang, S. Lv, Z. Lin and D. Tang, Biosens. Bioelectron., 2017, 95, 34-40.
- 82 G. Cai, Z. Yu, R. Ren and D. Tang, ACS Sens., 2018, 3, 632-
- 83 X. Zhang, F. Xu, B. Zhao, X. Ji, Y. Yao, D. Wu, Z. Gao and K. Jiang, Electrochim. Acta, 2014, 133, 615-622.
- 84 G.-L. Wang, K.-L. Liu, Y.-M. Dong, X.-M. Wu, Z.-J. Li and C. Zhang, *Biosens. Bioelectron.*, 2014, **62**, 66–72.
- 85 J. Ma, M. Zhang, W. Su, B. Wu, Z. Yang, X. Wang, B. Qiao, H. Pei, J. Tu, D. Chen and Q. Wu, Langmuir, 2022, 38, 751-761.
- 86 S. Siddiqui, S. Shawuti, Sirajuddin, J. H. Niazi and A. Qureshi, Ind. Eng. Chem. Res., 2019, 58, 8035-8043.
- 87 L. Meng, K. Xiao, X. Zhang, C. Du and J. Chen, Sens. Actuators B Chem., 2020, 305, 127480.
- 88 X. Xu, D. Liu, L. Luo, L. Li, K. Wang and T. J. S. You, Sens. Actuators B Chem., 2017, 251, 564-571.
- 89 Z. Yang, Y. Wang and D. Zhang, Sens. Actuators B Chem., 2018, 261, 515-521.
- 90 J. Song, J. Wang, X. Wang, W. Zhao, Y. Zhao, S. Wu, Z. Gao, J. Yuan and C. Meng, Biosens. Bioelectron., 2016, 80, 614-620.
- 91 G.-C. Fan, X.-L. Ren, C. Zhu, J.-R. Zhang and J.-J. Zhu, Biosens. Bioelectron., 2014, 59, 45-53.
- 92 H. Wang, H. Ye, B. Zhang, F. Zhao and B. Zeng, J. Phys. Chem. C, 2018, 122, 20329-20336.
- 93 D.-M. Han, L.-Y. Jiang, W.-Y. Tang, J.-J. Xu and H.-Y. Chen, Electrochem. Commun., 2015, 51, 72-75.